

Reconsidering Degeneration of Token Embeddings with Definitions for Encoder-based Pre-trained Language Models

Ying Zhang¹, Dongyuan Li², and Manabu Okumura^{1,3}

¹RIKEN Center for Advanced Intelligence Project

²Tokyo University

³Tokyo Institute of Technology

ying.zhang@riken.jp lidy94805@gmail.com oku@lr.pi.titech.ac.jp

Abstract

Learning token embeddings based on token co-occurrence statistics has proven effective for both pre-training and fine-tuning in natural language processing. However, recent studies have pointed out that the distribution of learned embeddings degenerates into anisotropy (*i.e.*, non-uniform distribution), and even pre-trained language models (PLMs) suffer from a loss of semantics-related information in embeddings for low-frequency tokens. This study first analyzes the fine-tuning dynamics of encoder-based PLMs and demonstrates their robustness against degeneration. On the basis of this analysis, we propose DefinitionEMB, a method that utilizes definitions to re-construct isotropically distributed and semantics-related token embeddings for encoder-based PLMs while maintaining original robustness during fine-tuning. Our experiments demonstrate the effectiveness of leveraging definitions from Wiktionary to re-construct such embeddings for two encoder-based PLMs: RoBERTa-base and BART-large. Furthermore, the re-constructed embeddings for low-frequency tokens improve the performance of these models across various GLUE and four text summarization datasets.¹

1 Introduction

Word embeddings, served as the foundation for various NLP tasks, represent word information using low-dimensional vectors (Parsing, 2009; Turian et al., 2010).² To learn precise syntactic and semantic embeddings, the predominant approach is to train models based on word co-occurrence statistics (Mikolov et al., 2013). Recent studies have highlighted that learned embeddings suffer from representation degeneration issues: 1) *Globally, the geometric distribution of the embedding matrix exhibits a narrow cone shape* (Gao et al., 2019). 2)

¹Our code will be available at Github.

²Please note that the embeddings discussed in this paper are the input to a model, distinct from the contextualized representations (*i.e.*, the hidden states) in subsequent layers.

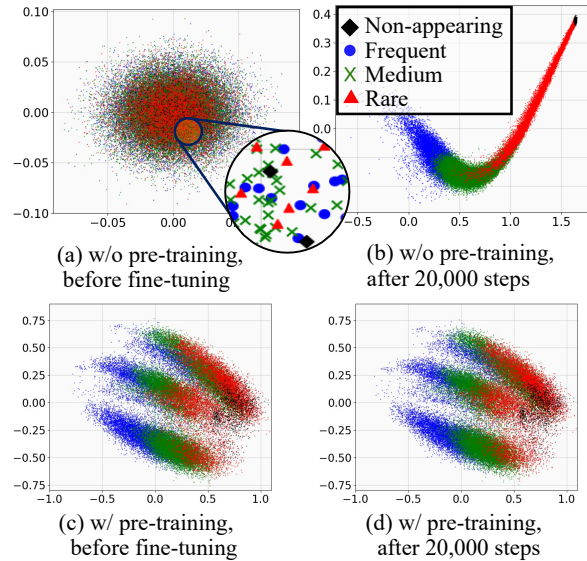


Figure 1: Transformer’s token embeddings with (w/) or without (w/o) pre-trained parameters during fine-tuning on the CNNDM dataset. Tokens are divided into four groups according to their frequency. (a) Isotropic distribution. (b) Narrow cone-shaped anisotropy. (c-d) BART’s embeddings shape remains unchanged, indicating its robustness against degeneration into a cone.

Locally, frequency-related embeddings are often mapped to the same region, making them indistinguishable and semantically unrelated (Yu et al., 2022). For more easily understanding the degeneration, we used SVD to project an embedding matrix of Transformer (Vaswani et al., 2017) into a two-dimensional space. Figure 1(a) shows the distribution of the initial embeddings is isotropic (*i.e.*, angularly uniform) and frequency-irrelevant. However, as shown in Figure 1(b), after learning task-specific embeddings, the shape changes into a narrow cone, and frequency-related embeddings are grouped together. The main reason is that the co-occurring tokens are trained to have similar representations, and other tokens are pushed in the opposite direction (Tissier et al., 2017; Mu et al., 2018; Demeter

et al., 2020). As a result, the expressiveness of the embedding matrix is reduced, leading to inferior performance in downstream tasks (Biś et al., 2021).

Previous studies have proposed solutions to alleviate the degeneration by post-processing embeddings or enhancing model optimization (Mu et al., 2018; Gong et al., 2018; Yu et al., 2022). However, these methods either handle word-level embeddings or fail to learn semantics-related embeddings for low-frequency (rare) subword tokens. This leaves the degeneration issue in token-level embeddings unsolved, particularly in pre-trained language models (PLMs) (Schick and Schütze, 2020). Currently, PLMs with token-level vocabularies have become dominant in many NLP tasks due to their plug-and-play convenience and outstanding efficacy. To improve the generalization of PLMs, it is essential to explore strategies for re-constructing their embeddings. To achieve this goal, this research focuses on encoder-based PLMs, including PLMs with encoder-only and encoder-decoder Transformer architectures, by first analyzing their behavior. Figure 1(c) shows that, unlike training from scratch, the encoder-decoder PLM, BART (Lewis et al., 2020), is robust against degeneration into a cone shape during fine-tuning. However, its pre-trained embeddings are still not ideally isotropic, with frequency-related embeddings mapped to the same region and rare tokens lacking semantics (Additional evidence is presented in § 4).

Given this, a natural question arises: *how can embeddings be re-constructed for encoder-based PLMs to preserve the semantics of rare tokens, achieve isotropic distribution, and maintain robustness against degeneration during fine-tuning?* To preserve the semantics of rare tokens, this paper proposes DefinitionEMB to re-construct their embeddings by leveraging corresponding dictionary definitions (e.g., Wiktionary). Moreover, to realize effective and robust re-construction for PLMs’ token-level vocabularies, DefinitionEMB uses a denoising autoencoder (Vincent et al., 2010) and is designed as an architecture-agnostic model that can be easily initialized from the given PLMs. To achieve isotropic distribution across appropriate semantic regions while being robust against degeneration during fine-tuning, DefinitionEMB is trained through mimicking (Pinter et al., 2017) well-learned embeddings. Our main contributions are summarized as follows:

- **Insights into Degeneration.** We observe that, although encoder-based PLMs do not degenerate

into a narrow cone during fine-tuning, their pre-trained embeddings are not ideally isotropic, with frequency-related embeddings mapped to the same semantic regions. Additionally, merely improving isotropy for encoder-based PLMs does not guarantee semantically distributed embeddings but instead can lead to further degeneration (§ 4).

- **Embeddings against Degeneration.** To the best of our knowledge, DefinitionEMB is the first method to re-construct pre-trained token embeddings for encoder-based PLMs being (1) isotropically distributed and semantics-related before fine-tuning, and (2) robust against degeneration into a cone shape during fine-tuning (§ 5).

- **Empirical Validation.** Extensive experiments across GLUE and four text summarization datasets demonstrate the effectiveness of DefinitionEMB for RoBERTa-base and BART-large PLMs (§ 6).

2 Related Work

Distribution of Embeddings. Various studies have attempted to improve the distribution of word/token embeddings. For example, to geometrically merge embeddings of popular (high-frequency) and rare words, Gong et al. (2018) utilized a discriminator of generative adversarial networks to classify embeddings as belonging to popular or rare words. Yu et al. (2022) proposed to gate the gradients of rare token embeddings to reduce degeneration into a narrow cone during training. To achieve isotropically distributed embeddings, Gao et al. (2019) and Zhang et al. (2020) minimized the distance between any two word embeddings. Other studies (Mu et al., 2018; Rajaei and Pilehvar, 2021; Biś et al., 2021) investigated the effectiveness of eliminating the common vector from specific groups of embeddings. *Compared to previous studies, our research considers both semantic and distributional information for embeddings. It is also the first to apply such considerations to improve the fine-tuned performance of PLMs, whose vocabulary consists of tokenized subwords.*

Learning Word Embeddings. Learning embeddings for specific words has been discussed for a long time. Previous studies have explored various solutions, such as leveraging surface-form information (Luong et al., 2013; Pinter et al., 2017; Sasaki et al., 2019) or the contexts in which these words occur (Khodak et al., 2018; Liu et al., 2019). Lexical definitions have also been considered to incorporate semantics-related information. For instance,

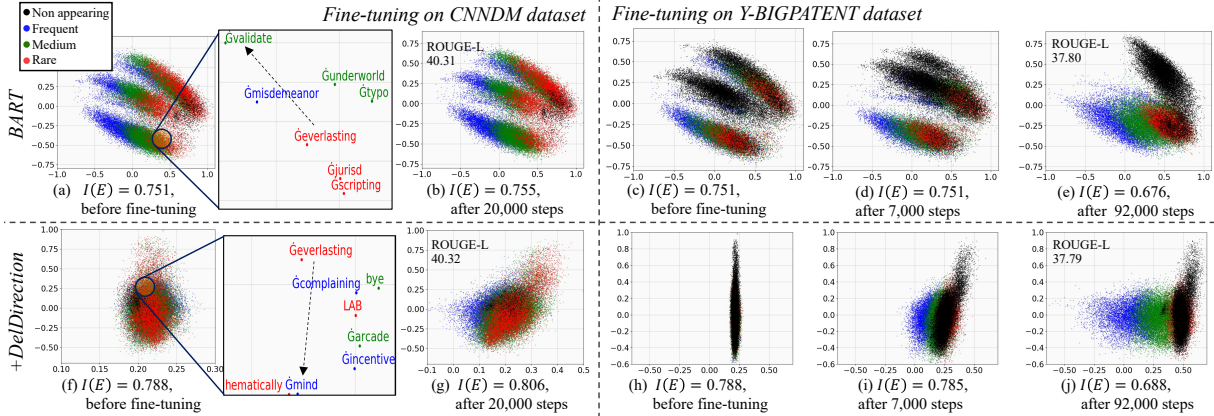


Figure 2: Token embeddings projected onto first two singular vectors. **Top**: During fine-tuning, BART’s embeddings with different frequencies maintain their distance and are robust against degeneration into a cone shape. **Bottom**: DelDirection causes higher-frequency tokens to drift farther away from their original positions, leading to a narrow cone shape. The dashed lines in (a) from “Geverlasting” point to its semantics-related tokens, recognized by both ChatGPT 3.5 (Achiam et al., 2023) and Claude 3 Haiku (Anthropic, 2024). Appendix D lists their recognition.

Tissier et al. (2017) utilized definitions to bring semantically related words closer. Various one-to-one mapping methods have also been proposed to construct embeddings for full words from corresponding definitions (Bahdanau et al., 2018; Zhang et al., 2021; Ruzzetti et al., 2022). *In contrast, we explore a one-to-many mapping, i.e., using a single definition to construct multiple token embeddings. Thus, our re-constructed embeddings can be easily applied to PLMs with token-level vocabularies.*

Representations in PLMs. There have also been studies that extend PLM’s embeddings or analyze contextualized word representations in PLMs. Chen et al. (2022) and Liang et al. (2023) extended embeddings of BERT for out-of-vocabulary words. Ethayarajh (2019) analyzed the isotropic distribution of several PLMs’ contextualized word representations (*i.e.*, hidden states) across model layers. These studies are out scope of this work.

3 Preliminaries

Let $\mathcal{V} = \{v_n\}_{n=1}^{|\mathcal{V}|}$ denote the predefined restricted vocabulary of a PLM, where $|\mathcal{V}|$ tokens are ranked in *descending order* according to their frequencies in pre-trained datasets. $\mathbf{E} \in \mathbb{R}^{|\mathcal{V}| \times h_e}$ denotes the pre-trained token embedding matrix, where h_e is the embedding size. Given a word w , we assume that w is tokenized into K tokens $(v_{w,1}, \dots, v_{w,K})$, and $\mathbf{e}(v) \in \mathbb{R}^{h_e}$ denotes the embedding of token v .

The geometry of \mathbf{E} is assumed to capture linguistic regularities, *i.e.*, the similarity between token embeddings reflects the semantic similarity of the

corresponding tokens. Therefore, researchers expect \mathbf{E} to exhibit a uniform distribution, denoted as isotropic, to maximize the containment of linguistic information for distinguishing tokens. To estimate isotropy, Mu et al. (2018) proposed the metric $I(\mathbf{E}) \in [0, 1]$, where a value closer to 1 indicates higher isotropy. They also proposed a post-processing technique to improve isotropy for \mathbf{E} by eliminating the common mean vector and top- β dominating directions from \mathbf{E} . We denote this method as *DelDirection* and consider it as a baseline with $\beta=10$. Appendix A shows more details.

4 Token Embedding Dynamics: An Experimental Investigation

Inspired by Yu et al. (2022)’s observation that Transformer exhibits narrow cone-shaped degeneration due to the unbalanced token frequency, we investigated whether token frequency influences the embedding of PLMs during fine-tuning. We first classified tokens into appearing and non-appearing groups based on their appearance in the corresponding fine-tuning dataset. Then, 30%, 50%, and 20% appearing tokens in \mathcal{V} were assigned to the frequent, medium, and rare groups, respectively. The main paper primarily focuses on the BART-large model on the CNNNDM and Y-BIGPATENT datasets, where CNNNDM has a large unique appearing vocabulary, while Y-BIGPATENT has a small one. Appendices B and C show more details.

In Figure 2, we conclude that **the encoder-based PLM does not degenerate into a narrow cone; instead, it exhibits drift patterns influenced by to-**

ken frequency. Additionally, merely improving isotropy for it does not guarantee semantically distributed embeddings and does not improve performance for downstream tasks. We would like to share the following three main findings:

Finding-1. *The pre-trained embeddings of BART still suffer from anisotropy and a lack of semantics.* Before fine-tuning, BART achieves an $I(\mathbf{E})$ score of 0.751, suggesting room for improvement. The zoomed-in view in Figure 2 (a) further shows that rare tokens still lack sufficient semantic information, e.g., most neighbors of the rare token “Geverlasting” are semantically unrelated to it. This finding motivates us to incorporate semantics-related information and improve isotropy before fine-tuning to enhance downstream performance.

Finding-2. *Although using DelDirection before fine-tuning yields higher $I(\mathbf{E})$ and more thoroughly mixed embeddings, it leads to a fragile distribution and no further improved ROUGE (Lin, 2004) scores on the downstream datasets.* Specifically, as seen in Figures 2 (g) and (i), popular tokens drift away from the original overlapping position. After more updates, as seen in Figure 2 (j), tokens degenerate into a narrow cone with frequency bias. Finally, it does not improve model performance (i.e., ROUGE). This motivates us to investigate an effective method to alleviate degeneration during fine-tuning and improve performance.

Finding-3. *Figures 2 (b), (d), and (e) show that, while appearing and non-appearing tokens drift into different regions, BART is robust against degeneration into a cone shape with increasing number of updates.* This robustness is neither architecture- nor size-dependent, as RoBERTa-base exhibits similar robustness against degeneration (see Appendix C). This finding aligns with recent studies which suggest that fine-tuning rarely alters the majority of PLMs’ parameters (Jain et al., 2024; Panigrahi et al., 2023). These results motivate us to leverage the robustness of PLMs to prevent degeneration into a cone shape during fine-tuning.

5 Methodology

Let $f(\theta^{\text{PT}})$ be an encoder-based PLM with parameter θ^{PT} . As discussed in § 4, the pre-trained token embeddings \mathbf{E} of $f(\theta^{\text{PT}})$ suffer from anisotropy and a lack of semantics before fine-tuning. The re-constructed embeddings should also ensure robustness against degeneration during fine-tuning.

As shown in Figure 3, we introduce a novel framework **DefinitionEMB** to solve these issues by simply re-constructing token embeddings for \mathbf{E} from the corresponding word definition.

5.1 Semantic Embedding Re-construction

Recall that pre-trained embeddings of rare token still lack semantic information. Ausubel (1968) indicated that achieving a deep understanding of a new word involves linking it to already known relevant concepts. Motivated by this, DefinitionEMB connects tokens of a word to their corresponding dictionary definitions (e.g., Wiktionary). To help DefinitionEMB effectively understand semantics of rare tokens, we base our approach on a denoising autoencoder, which first corrupts a sequence into a noisy version and then re-constructs it back to a clean form (Vincent et al., 2010). Thus, embedding re-construction is realized as a cloze exercise, as shown in the left of Figure 3.

To form the cloze task, we first map a word w and its definition into a sentence, referred to as the full prompt p . Then, we randomly corrupt parts of tokens in the word w within the full prompt and train DefinitionEMB to re-construct the embeddings of these corrupted tokens. Note that in this example, “#” could be filled with multiple subwords tokens. Several tokens, such as “ags”, are randomly provided in the underline, with the underlined tokens “#ags#” corresponding to the target word “jags”. Since the embedding of the random token “ags” may be noisy, this denoising strategy helps to generate effective representations when facing noisy inputs. In addition, DefinitionEMB is designed as an architecture-agnostic model, that can be easily initialized from the given PLMs to leverage pre-trained parameters. We apply different corruption strategies based on model types: BERT-style masking (Devlin et al., 2019) for encoder-only PLMs and T5-style masking (Raffel et al., 2020) for encoder-decoder PLMs. Their effectiveness has been well demonstrated in prior studies (Voita et al., 2019; Raffel et al., 2020; Salazar et al., 2020).

Mathematically, let κ denote the set of corrupted positions, $p_\kappa \subseteq w$ the set of corrupted tokens, and $p_{\setminus\kappa}$ the corrupted prompt. Let $v_{p,i}$ represent the i^{th} token in prompt p . For a token $v_{p,k}$, where $k \in \kappa$, DefinitionEMB re-constructs its semantics-related definition embedding $\tilde{e}(v_{p,k})$ as follows:

$$\begin{aligned} \mathbf{s}_{g(k)} &= f(k, p_{\setminus\kappa}; \theta^{\text{PT}}), \\ \tilde{e}(v_{p,k}) &= \mathbf{W}\mathbf{s}_{g(k)}, \end{aligned} \quad (1)$$

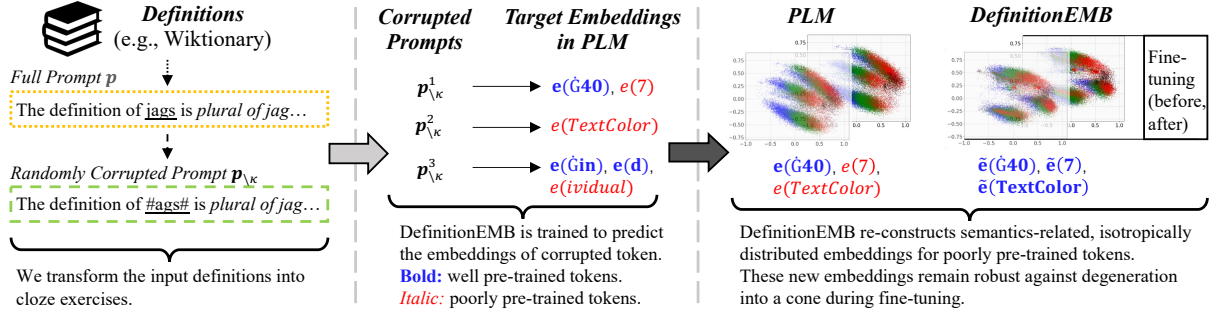


Figure 3: Overview of constructing definition embeddings to replace pre-trained embeddings.

where $\mathbf{s}_{g(k)} \in \mathbb{R}^{h_s}$ is the last hidden state at position $g(k)$ and $\mathbf{W} \in \mathbb{R}^{h_e \times h_s}$ is a weight matrix. The function $g(\cdot)$ maps the corrupted position to the prediction position. For an encoder-only PLM, $g(k) = k$. For an encoder-decoder PLM, $g(k)$ refers to the position of the delimiter in front of v_k in the decoder. Appendix E.1 explains our methods for generating and corrupting prompts, and $g(\cdot)$.

5.2 Robustness against Degeneration

Definitions tend to contain popular and easily understandable words to explain their corresponding target words. Thus, the pre-trained embeddings for most tokens in the cloze exercise can be isotropically distributed and semantics-related. DefinitionEMB is, therefore, trained using a mimicking approach (Pinter et al., 2017), which optimizes embeddings by matching the predicted embeddings to well pre-trained ones. Through finding the overall optimal embedding space for the PLM’s vocabulary \mathcal{V} , DefinitionEMB learns a transformation function from ideally distributed input embeddings to target embeddings. This approach ensures that the re-constructed embeddings of poorly pre-trained tokens are uniformly distributed across appropriate semantic regions while being robust against degeneration during fine-tuning. Next, we discuss how to identify well pre-trained embeddings. Someone might consider directly adopting embeddings of high-frequency tokens. However, we argue that embeddings of rare tokens may also contain useful information. Therefore, following Burns et al. (2023), we incorporate definitions involving all tokens in \mathcal{V} for training, allowing the model to automatically identify well pre-trained embeddings.

Let $\mathcal{D} = \{(\mathbf{w}^m, \mathbf{p}^m)\}_{m=1}^M$ denote a corpus with M word-definition pairs. For $v_{\mathbf{p}^m, k}$, DefinitionEMB is optimized by minimizing the mean squared error between pre-trained embeddings $e(v_{\mathbf{p}^m, k})$ and definition embeddings $\tilde{e}(v_{\mathbf{p}^m, k})$ as:

$$\mathcal{L} = \sum_{m=1}^M \frac{\sum_{k \in \kappa^m} \|e(v_{\mathbf{p}^m, k}) - \tilde{e}(v_{\mathbf{p}^m, k})\|^2}{M|\kappa^m|}, \quad (2)$$

where $|\kappa^m|$ is the number of corrupt tokens for \mathbf{p}^m .

5.3 Replacing Strategy in Inference

Given a specific downstream task, we first remove tokens from \mathcal{V} that do not appear in the corresponding fine-tuning dataset. The remaining set of tokens is denoted as $\mathcal{V}_{[task]}$, where the tokens in $\mathcal{V}_{[task]}$ are ranked in *descending order* according to their frequency in the dataset for pre-training. Our preliminary experiments in Appendix E.2 demonstrate that, when replacing 5% of the last tokens in $\mathcal{V}_{[MRPC]}$, BART achieves the highest accuracy compared to replacing random or top tokens in $\mathcal{V}_{[MRPC]}$ on MRPC dataset. Therefore, as an initial study on re-constructing token embeddings for PLMs, this study focuses on low-frequency tokens. Our replacing strategy has the following definition.

Definition 1 For any PLMs with diverse data distributions and task requirements for downstream tasks, we replace $\min(\alpha\% * |\mathcal{V}|, |\mathcal{V}_{[task]}|)$ of the last tokens in $\mathcal{V}_{[task]}$, where α is a hyperparameter.

Based on Definition 1, before fine-tuning, we straightforwardly replace $\min(\alpha\% * |\mathcal{V}|, |\mathcal{V}_{[task]}|)$ pre-trained embeddings with definition embeddings as $e(v) = \tilde{e}(v)$, which can avoid missing definition information or excessive noise in $e(v)$.

6 Experiments

Following Mu et al. (2018) and Lewis et al. (2020), we assessed the performance of PLMs with diverse embeddings on various benchmark tasks, including embeddings isotropy, word similarity, and natural language understanding on the General Language Understanding Evaluation (GLUE) benchmark. Additionally, for the encoder-decoder PLM, we tested its performance with replaced embeddings on the text summarization task to evaluate

Model	$I(\mathbf{E}) \uparrow$			
	Frequent	Medium	Rare	All Tokens
RoBERTa	0.694	0.501	0.315	0.504
+ DelDirection	0.639	0.641	0.599	0.624
+ DefinitionEMB	0.649	0.470	0.382	0.519
BART	0.851	0.668	0.515	0.751
+ DelDirection	0.790	0.775	0.731	0.788
+ DefinitionEMB	0.834	0.800	0.603	0.876

Table 1: Isotropy of \mathbf{E} . The frequent (30%), medium (50%), and rare (20%) groups are determined based on the token index in \mathcal{V} . Appendix G.1 shows projected \mathbf{E} .

both its text comprehension and generation capabilities. Specifically, GLEU and text summarization evaluated the fine-tuned performance of PLMs.

6.1 Experimental Settings

For different downstream tasks, we used various datasets, as described in the following experimental sections. The statistics for these datasets are described in Appendix B. We adopted token-level DelDirection (Mu et al., 2018) as our baseline since all other post-processing methods focused on word-level degeneration issues and could not be applied to PLMs. We adopted the RoBERTa-base and BART-large models as our backbone PLMs with encoder-only and encoder-decoder architectures, respectively. Both backbones used the same vocabulary \mathcal{V} with size $N = 50,265$. Appendix F lists the hyperparameter settings, tuning³ for DefinitionEMB, and fine-tuning PLMs for downstream tasks. Scores are the average over three trials.

We used 1.5G English-language Wiktionary as definitions to train DefinitionEMB. The 1,464,327 extracted definitions were randomly divided into 1,454,327 for training and 10,000 for validation. We also extracted 1,388 definitions from the Internet used for numbers and named entity tokens. Overall, 1,455,715 examples were used for training DefinitionEMB. During inference, these examples were reused for loading definition embeddings. Once a token embedding has been replaced, it will not be replaced during the rest of the procedure. 2,305 tokens from \mathcal{V} were always excluded from replacement because they did not have a corresponding definition, such as “)= (“.

6.2 Quantitative Evaluation

► **Initial Isotropy.** We measured the initial isotropy of token embeddings \mathbf{E} in PLMs and the isotropy after completely replacing \mathbf{E} . Table 1

³We tuned α on the validation set.

Model	Spearman Score \uparrow				
	RG65	RW	SimLex	SimVerb	Ave
RoBERTa	16.05	18.89	26.67	11.81	18.36
+ DefinitionEMB	18.88	18.96	27.15	11.91	19.23
BART	15.32	19.66	28.56	13.09	19.16
+ DefinitionEMB	15.67	19.76	28.63	12.72	19.20

Table 2: Results on the word similarity task with dot product. DefinitionEMB completely replaced \mathbf{E} . Appendix G.3 shows the results with cosine similarity.

shows that both RoBERTa and BART exhibit high isotropy in the frequent group but low isotropy in the rare group. DelDirection helps achieve a uniformly distributed isotropy across frequency groups and results in the highest isotropy for the rare group, although it decreases isotropy in the frequent group. DefinitionEMB also showcases a more uniform isotropy distribution than the original PLMs, displaying a lower isotropy for the frequent group but higher isotropy for the rare group. Additionally, DefinitionEMB for BART achieves the highest isotropy for the medium group as well as for the entire \mathbf{E} . Appendix G.2 analyzes differences of using DefinitionEMB on BART and RoBERTa due to the different distribution of pre-trained embeddings and used masking strategies.

► **Word Similarity.** Compared to BART and RoBERTa, which utilize over 160 GB of contexts to learn semantic embeddings, DefinitionEMB utilizes definition information at only 1% of the size of their contexts. To evaluate the construction capabilities of DefinitionEMB on representations given such limited information, we adopted the word similarity task to investigate whether DefinitionEMB can maintain the original semantic relationships.⁴ Following Mu et al. (2018), we assessed whether the similarity between the embeddings of two given words aligns with the ground truth, in terms of Spearman’s rank correlation. We used the dot product to measure the similarity between word embeddings across four datasets: RG65, rare-words (RW), SimLex-999, and SimVerb-3500. We estimated the word embeddings by summing the embeddings of the corresponding tokens. As Table 2 shows, using DefinitionEMB yields higher Spearman scores than the original PLMs on the RG65, SimLex-999, and RW datasets. In particular, the results of the RW dataset, which consists of only rare words, underscore the effectiveness of DefinitionEMB in

⁴DelDirection was excluded because it does not construct representations but rather updates existing embeddings.

Model	SST	MRPC	STS	QQP	MNLI		QNLI	RTE	Average
					m	mm			
RoBERTa	95.7	87.5	89.6 / 89.0	89.6	87.3	86.7	93.1	73.9	88.0
+ DelDefinition	95.9	86.9	89.0 / 88.3	89.3	87.3	86.8	93.0	72.3	87.6
+ DefinitionEMB	95.9	87.7	89.6 / 89.0	89.4	87.6	87.0	93.0	75.3	88.3
BART	96.5	87.8	91.2 / 90.6	90.1	90.0	89.2	94.7	82.4	90.3
+ DelDefinition	96.4	87.3	90.9 / 90.4	89.9	89.9	89.2	94.7	78.7	89.7
+ DefinitionEMB	96.4	88.3	91.3 / 90.7	90.1	90.0	89.2	94.9	83.3	90.5

Table 3: Experimental results on GLUE. For the STS dataset, we report the Pearson/Spearman’s rank correlation, while for other datasets, we report accuracy scores. For the MNLI dataset, we report results for Matched (m) and Mismatched (mm) sets. Appendix G.4 describes corresponding $I(\mathbf{E})$.

Model	CNNDM	Y-BIGPATENT	XSum	Billsum	Average
BART	43.57 / 20.93 / 40.31	43.96 / 18.92 / 37.80	43.76 / 20.40 / 34.65	51.02 / 32.44 / 39.11	45.58 / 23.17 / 37.97
+DelDirection	43.59 / 20.93 / 40.32	43.91 / 18.85 / 37.79	43.90 / 20.58 / 34.86	50.89 / 32.22 / 38.97	45.57 / 23.15 / 37.99
+DefinitionEMB	43.78 † / 20.94 / 40.52 ‡	44.16 ‡ / 19.06 ‡ / 38.01 ‡	43.96 † / 20.61 † / 34.87 †	50.96 / 32.64 ‡ / 39.28	45.72 / 23.31 / 38.17

Table 4: Experimental results (ROUGE1-F1 / ROUGE2-F1 / ROUGEL-F1) on the text summarization tasks. † and ‡ indicate that the score is significantly superior to BART with a p-value < 0.01 and < 0.05, respectively.

capturing the semantic information for these words. **> GLUE.** We conducted experiments on the GLUE benchmark (Wang et al., 2018) across seven datasets: SST, MRPC, STS, QQP, MNLI, QNLI, and RTE. Table 3 reports our test set results obtained from the public leaderboard.⁵ Using DelDirection results in the lowest accuracy and Pearson/Spearman’s rank correlation in most cases; however, it achieves the highest $I(\mathbf{E})$ across all datasets, as listed in Appendix G.4. This supports our assumption that DelDirection focuses on the global isotropic distribution of embeddings at the expense of semantic information. In contrast, DefinitionEMB improves both the global distribution and downstream performance on GLUE, particularly for the MRPC and RTE datasets. This improvement highlights DefinitionEMB’s advantage in enhancing semantic information, as these tasks contain low-frequency tokens that suffer from insufficient fine-tuning, thus increasing the necessity for replacing their embeddings.⁶

> Text Summarization. For the downstream summarization task, we used public abstractive summarization datasets, including CNN/DailyMail (CNNDM), Extreme Summarization (XSum), BillSum, and Y-BIGPATENT. We evaluated the model

⁵<https://gluebenchmark.com/>

⁶While the STS task also involves low-frequency tokens, it primarily requires an understanding of popular words, such as the distinction between “woman” and “man”. In contrast, MRPC and RTE involve the comprehension of more complex sentences. This difference explains why DefinitionEMB does not show the same level of improvement across these tasks.

Models	ROUGE (F1) ↑		
	ROUGE-1	ROUGE-2	ROUGE-L
BART	34.99	14.67	32.19
+DelDirection	35.13 (+0.14)	15.05 (+0.38)	32.33 (+0.14)
+DefinitionEMB	36.11 †(+1.12)	15.75 †(+1.08)	33.44 ‡(+1.25)

Table 5: Experimental results on the CNNDM subset for rare tokens (index > 40,000 in \mathcal{V}). (+scores) indicates the improvement compared to BART.

performance on these datasets using the ROUGE scores and compared BART + DefinitionEMB with the original BART using paired bootstrap resampling (Koehn, 2004) for the significance test. Table 4 shows that using DelDirection improves the ROUGEL-F1 score by 0.21 points for BART on the XSum dataset. However, the difference between BART and DelDirection is very limited in other datasets; DelDirection achieves even a lower ROUGEL-F1 score, with a decrease of 0.14 points, than BART on the Billsum dataset. In contrast, by improving semantics-related information and frequency-aware $I(\mathbf{E})$ for rare tokens, DefinitionEMB achieves the highest ROUGEL-F1 scores, with improvements of 0.21, 0.21, 0.22, and 0.17 points on the CNNDM, Y-BIGPATENT, XSum, and Billsum datasets, respectively, for BART.

6.3 Analysis of DefinitionEMB

> Ablation Study. Appendix G.5 analyzes the effectiveness of replacing only appearing tokens instead of all tokens. To evaluate DefinitionEMB’s ability to handle rare tokens, we conducted ex-

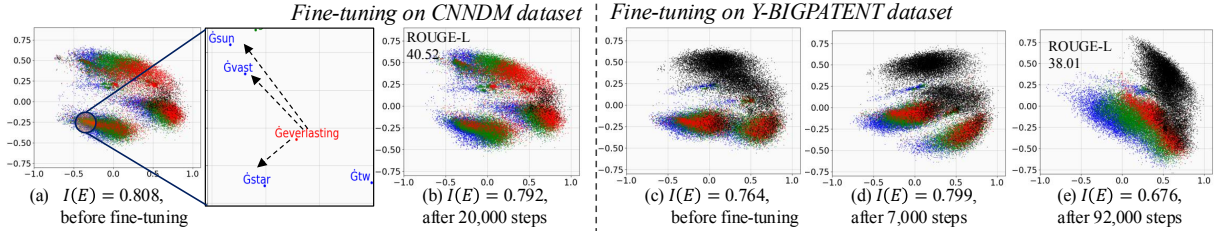


Figure 4: Projected token embeddings in BART+DefinitionEMB before and after fine-tuning. Embeddings with different frequencies maintain their distance during fine-tuning, demonstrating robustness against degeneration. The embeddings in (a) and (c) exhibit different shapes due to the different α .

Models	Acc.↑
BART	96.4
+DelDirection	84.8
+DefinitionEMB	98.3

(a) Probing results.

Reference: Marvel Studios ... Age of Ultron ... Daredevil costume. X-Men Apocalypse Angel played by Ben Hardy.

BART: ... Age of Ultron sequel. The actor has been playing the android for many years in the comics. ...

+DelDirection: ... Age of Ultron is finally revealed. ...

+DefinitionEMB: ... Age of Ultron sequel. Marvel Studios also announced a new character for X-Men: Apocalypse Ben Hardy will play the winged mutant Angel in X-Men: Apocalypse, Director Bryan Singer said.

(b) Generated summarization.

Figure 5: Case study on the CNNDM dataset. (a) Probing results. (b) Example generated summaries. Underline indicates the rare tokens with index larger than 40,000 in \mathcal{V} . Appendix H.2 includes a full version.

periments on 65 data pairs of the CNNDM test set, whose target sentence consisted of a high proportion of rare tokens (at least 5%). Details of this subset are provided in Appendix F. As shown in Table 5, DefinitionEMB achieves superior scores, with improvements of over 1 point across all ROUGE metrics, compared to BART, while DelDirection improves only ROUGE1 and ROUGE2 by 0.14 points. These results highlight the effectiveness of DefinitionEMB and show that DelDirection, as an update method rather than a construction method for embeddings, is less effective for rare tokens on downstream tasks.

► **Embedding Dynamics.** Figure 4 depicts the projected token embeddings of DefinitionEMB. On the CNNDM dataset, tokens exhibit minimal drift from “before” to “after” fine-tuning. Conversely, on the Y-BIGPATENT dataset, tokens within the same group move together after fine-tuning. These findings align with those of BART in Figure 2, indicating that using DefinitionEMB helps maintain BART’s robustness against degeneration into a narrow cone. Additionally, using DefinitionEMB before fine-tuning increases $I(\mathbf{E})$ for BART across the CNNDM and Y-BIGPATENT datasets. It supports our observation that, compared to BART, embeddings in BART+DefinitionEMB with different frequencies are more thoroughly mixed.

► **Probing Semantics.** Zooming in Figure 4 (a)

reveals that the token “Geverlasting” is surrounded by more semantically related tokens than BART with and without DelDirection before fine-tuning (Figure 2). This case study demonstrates that using DefinitionEMB provides more semantically related information in the initial step (*i.e.*, the input layer). To investigate whether a model can encode and extract such semantic information in subsequent layers, we followed Allen-Zhu and Li (2024) and conducted a simple probing test. We froze each CNNDM fine-tuned model and trained a classifier to classify the last layer’s hidden states of input words as “numeric < 1,000”, “numeric > 1,000”, or “others”. In inference, we evaluated accuracy on 78 rare numeric tokens and 78 rare non-numeric tokens. Higher accuracy indicates a stronger link to the token’s semantics. The overall accuracy is shown in Figure 5 (a). Using BART+DefinitionEMB achieves the highest accuracy at 98.3%, demonstrating that it encodes and extracts more semantic information. Appendix H.1 shows more details.

7 Conclusion

This research found that during fine-tuning, the embeddings of the encoder-based PLMs do not degenerate into a narrow cone in a low-dimensional space. However, eliminating specific directions from embeddings to ensure isotropy leads to loss of semantics and further degeneration. Experimental results demonstrated that using DefinitionEMB for PLMs, RoBERTa and BART, improves the distribution of embeddings and enables low-frequency token embeddings to retain semantics-related information before fine-tuning. These new embeddings also maintained PLMs’ robustness against degeneration and led to improved downstream performance. Considering the recent emergence of understanding the internal workings of language models, this research paves the way for future work to explore why PLMs are robust against degeneration.

Limitations

Limited Models. The scope of this paper is limited to encoder-based PLMs. Although DefinitionEMB can yield effective embeddings for these models by the reconstruction, its denoising autoencoder-based objective function makes it challenging to directly apply it to decoder-only PLMs. This is because decoder-only PLMs use standard causal language modeling (left-to-right), which causes different information flow across layers compared to the masked language modeling, utilized in DefinitionEMB (Voita et al., 2019). While we aimed to emphasize the effectiveness of definition datasets in addressing degeneration for PLMs, future work could explore methods that can be effectively applied to decoder-only PLMs, especially large-scale ones.

Limited Understanding of PLMs’ Robustness. One of our findings is that encoder-based PLMs do not degenerate into a cone shape during fine-tuning. While this finding aligns with recent studies that PLMs rarely alter their parameters during fine-tuning (Jain et al., 2024; Panigrahi et al., 2023), it tells only half the story — modifying model parameters before fine-tuning can lead to more effective performance. However, to fully understand why PLMs’ embeddings are robust against degeneration during fine-tuning and to pinpoint improvements in the models, the interplay between embedding layers and other components of the model architecture, such as attention layers, could be further studied.

Acknowledgements

We thank Prof. Min-Yen Kan for suggesting the types of rare tokens to us. We thank Prof. Keisuke Sakaguchi and Prof. Sho Yokoi for their suggestions on the writing.

References

- Josh Achiam, Steven Adler, Sandhini Agarwal, et al. 2023. [Gpt-4 technical report](#). *arXiv preprint arXiv:2303.08774*.
- Zeyuan Allen-Zhu and Yuanzhi Li. 2024. [Physics of language models: Part 3.1, knowledge storage and extraction](#). In *Forty-first International Conference on Machine Learning*.
- Anthropic. 2024. [The claude 3 model family: Opus, sonnet, haiku](#). *Technique Report from Website*.
- David Paul Ausubel. 1968. *Educational psychology: A cognitive view*. Holt, Rinehart and Winston.
- Dzmitry Bahdanau, Tom Bosc, Stanisław Jastrzębski, Edward Grefenstette, Pascal Vincent, and Yoshua Bengio. 2018. [Learning to compute word embeddings on the fly](#). *arXiv preprint arXiv:1706.00286*.
- Daniel Biś, Maksim Podkorytov, and Xiuwen Liu. 2021. [Too much in common: Shifting of embeddings in transformer language models and its implications](#). In *Proceedings of the 2021 Conference of the North American Chapter of the Association for Computational Linguistics: Human Language Technologies*, pages 5117–5130.
- Collin Burns, Haotian Ye, Dan Klein, and Jacob Steinhardt. 2023. [Discovering latent knowledge in language models without supervision](#). In *The Eleventh International Conference on Learning Representations*.
- Xingyu Cai, Jiaji Huang, Yuchen Bian, and Kenneth Church. 2021. [Isotropy in the contextual embedding space: Clusters and manifolds](#). In *International Conference on Learning Representations*.
- Lihu Chen, Gael Varoquaux, and Fabian Suchanek. 2022. [Imputing out-of-vocabulary embeddings with LOVE makes LanguageModels robust with little cost](#). In *Proceedings of the 60th Annual Meeting of the Association for Computational Linguistics (Volume 1: Long Papers)*, pages 3488–3504, Dublin, Ireland. Association for Computational Linguistics.
- David Demeter, Gregory Kimmel, and Doug Downey. 2020. [Stolen probability: A structural weakness of neural language models](#). In *Proceedings of the 58th Annual Meeting of the Association for Computational Linguistics*, pages 2191–2197.
- Jacob Devlin, Ming-Wei Chang, Kenton Lee, and Kristina Toutanova. 2019. [BERT: Pre-training of deep bidirectional transformers for language understanding](#). In *Proceedings of the 2019 Conference of the North American Chapter of the Association for Computational Linguistics: Human Language Technologies*, pages 4171–4186.
- Kawin Ethayarajh. 2019. [How contextual are contextualized word representations? Comparing the geometry of BERT, ELMo, and GPT-2 embeddings](#). In *Proceedings of the 2019 Conference on Empirical Methods in Natural Language Processing and the 9th International Joint Conference on Natural Language Processing (EMNLP-IJCNLP)*, pages 55–65, Hong Kong, China. Association for Computational Linguistics.
- Jun Gao, Di He, Xu Tan, et al. 2019. [Representation degeneration problem in training natural language generation models](#). In *International Conference on Learning Representations*.
- Daniela Gerz, Ivan Vulić, Felix Hill, Roi Reichart, and Anna Korhonen. 2016. [SimVerb-3500: A large-scale](#)

- evaluation set of verb similarity. In *Proceedings of the 2016 Conference on Empirical Methods in Natural Language Processing*, pages 2173–2182.
- Chengyue Gong, Di He, Xu Tan, Tao Qin, Liwei Wang, and Tie-Yan Liu. 2018. **Frage: Frequency-agnostic word representation**. In *Advances in Neural Information Processing Systems*, volume 31.
- Karl Moritz Hermann, Tomas Kocisky, Edward Grefenstette, et al. 2015. **Teaching machines to read and comprehend**. In *Advances in Neural Information Processing Systems*, volume 28.
- Felix Hill, Roi Reichart, and Anna Korhonen. 2015. **SimLex-999: Evaluating semantic models with (genuine) similarity estimation**. *Computational Linguistics*, 41(4):665–695.
- Rob J Hyndman and George Athanasopoulos. 2018. *Forecasting: principles and practice*. OTexts.
- Samyak Jain, Robert Kirk, Ekdeep Singh Lubana, Robert P. Dick, Hidenori Tanaka, Tim Rocktäschel, Edward Grefenstette, and David Krueger. 2024. **Mechanistically analyzing the effects of fine-tuning on procedurally defined tasks**. In *The Twelfth International Conference on Learning Representations*.
- Mikhail Khodak, Nikunj Saunshi, Yingyu Liang, Tengyu Ma, Brandon Stewart, and Sanjeev Arora. 2018. **A la carte embedding: Cheap but effective induction of semantic feature vectors**. In *Proceedings of the 56th Annual Meeting of the Association for Computational Linguistics*, pages 12–22.
- Philipp Koehn. 2004. **Statistical significance tests for machine translation evaluation**. In *Proceedings of the 2004 Conference on Empirical Methods in Natural Language Processing*, pages 388–395.
- Anastassia Kornilova and Vladimir Eidelman. 2019. **BillSum: A corpus for automatic summarization of US legislation**. In *Proceedings of the 2nd Workshop on New Frontiers in Summarization*, pages 48–56.
- Mike Lewis, Yinhan Liu, Naman Goyal, et al. 2020. **BART: Denoising sequence-to-sequence pre-training for natural language generation, translation, and comprehension**. In *Proceedings of the 58th Annual Meeting of the Association for Computational Linguistics*, pages 7871–7880.
- Ziran Liang, Yuyin Lu, HeGang Chen, and Yanghui Rao. 2023. **Graph-based relation mining for context-free out-of-vocabulary word embedding learning**. In *Proceedings of the 61st Annual Meeting of the Association for Computational Linguistics (Volume 1: Long Papers)*, pages 14133–14149, Toronto, Canada. Association for Computational Linguistics.
- Chin-Yew Lin. 2004. **ROUGE: A package for automatic evaluation of summaries**. In *Text Summarization Branches Out*, pages 74–81.
- Qianchu Liu, Diana McCarthy, and Anna Korhonen. 2019. **Second-order contexts from lexical substitutes for few-shot learning of word representations**. In *Proceedings of the Eighth Joint Conference on Lexical and Computational Semantics (*SEM 2019)*, pages 61–67.
- Thang Luong, Richard Socher, and Christopher Manning. 2013. **Better word representations with recursive neural networks for morphology**. In *Proceedings of the Seventeenth Conference on Computational Natural Language Learning*, pages 104–113.
- Tomas Mikolov, Kai Chen, Greg Corrado, and Jeffrey Dean. 2013. **Efficient estimation of word representations in vector space**. *arXiv preprint arXiv:1301.3781*.
- Jiaqi Mu, Pramod Viswanath, and et al. 2018. **All-but-the-top: Simple and effective postprocessing for word representations**. In *International Conference on Learning Representations*.
- Shashi Narayan, Shay B. Cohen, and Mirella Lapata. 2018. **Don’t give me the details, just the summary! topic-aware convolutional neural networks for extreme summarization**. In *Proceedings of the 2018 Conference on Empirical Methods in Natural Language Processing*, pages 1797–1807.
- Myle Ott, Sergey Edunov, Alexei Baevski, et al. 2019. **fairseq: A fast, extensible toolkit for sequence modeling**. In *Proceedings of the 2019 Conference of the North American Chapter of the Association for Computational Linguistics*, pages 48–53.
- Abhishek Panigrahi, Nikunj Saunshi, Haoyu Zhao, and Sanjeev Arora. 2023. **Task-specific skill localization in fine-tuned language models**. In *Proceedings of the 40th International Conference on Machine Learning*, volume 202 of *Proceedings of Machine Learning Research*, pages 27011–27033. PMLR.
- Constituency Parsing. 2009. **Speech and language processing**. *Power Point Slides*.
- Yuval Pinter, Robert Guthrie, and Jacob Eisenstein. 2017. **Mimicking word embeddings using subword RNNs**. In *Proceedings of the 2017 Conference on Empirical Methods in Natural Language Processing*, pages 102–112.
- Ofir Press and Lior Wolf. 2017. **Using the output embedding to improve language models**. In *Proceedings of the 15th Conference of the European Chapter of the Association for Computational Linguistics: Volume 2, Short Papers*, pages 157–163.
- Colin Raffel, Noam Shazeer, Adam Roberts, et al. 2020. **Exploring the limits of transfer learning with a unified text-to-text transformer**. *The Journal of Machine Learning Research*, 21(1).
- Sara Rajae and Mohammad Taher Pilehvar. 2021. **A cluster-based approach for improving isotropy in contextual embedding space**. In *Proceedings of the 59th*

- Annual Meeting of the Association for Computational Linguistics and the 11th International Joint Conference on Natural Language Processing (Volume 2: Short Papers)*, pages 575–584.
- Herbert Rubenstein and John B. Goodenough. 1965. [Contextual correlates of synonymy](#). *Communications of the ACM*, 8(10):627–633.
- Elena Sofia Ruzzetti, Leonardo Ranaldi, Michele Tromattei, Francesca Fallucchi, Noemi Scarpato, and Fabio Massimo Zanzotto. 2022. [Lacking the embedding of a word? look it up into a traditional dictionary](#). In *Findings of the Association for Computational Linguistics: ACL 2022*, pages 2651–2662.
- Julian Salazar, Davis Liang, Toan Q. Nguyen, and Katrin Kirchhoff. 2020. [Masked language model scoring](#). In *Proceedings of the 58th Annual Meeting of the Association for Computational Linguistics*, pages 2699–2712, Online. Association for Computational Linguistics.
- Shota Sasaki, Jun Suzuki, and Kentaro Inui. 2019. [Subword-based Compact Reconstruction of Word Embeddings](#). In *Proceedings of the 2019 Conference of the North American Chapter of the Association for Computational Linguistics: Human Language Technologies*, pages 3498–3508.
- Timo Schick and Hinrich Schütze. 2020. [Rare words: A major problem for contextualized embeddings and how to fix it by attentive mimicking](#). In *Proceedings of the AAAI Conference on Artificial Intelligence*, volume 34, pages 8766–8774.
- Eva Sharma, Chen Li, and Lu Wang. 2019. [BIG-PATENT: A large-scale dataset for abstractive and coherent summarization](#). In *Proceedings of the 57th Annual Meeting of the Association for Computational Linguistics*, pages 2204–2213.
- Julien Tissier, Christophe Gravier, and Amaury Habrard. 2017. [Dict2vec : Learning word embeddings using lexical dictionaries](#). In *Proceedings of the 2017 Conference on Empirical Methods in Natural Language Processing*, pages 254–263.
- Joseph Turian, Lev-Arie Ratinov, and Yoshua Bengio. 2010. [Word representations: A simple and general method for semi-supervised learning](#). In *Proceedings of the 48th Annual Meeting of the Association for Computational Linguistics*, pages 384–394.
- Ashish Vaswani, Noam Shazeer, Niki Parmar, et al. 2017. [Attention is all you need](#). In *Advances in Neural Information Processing Systems*, volume 30.
- Pascal Vincent, Hugo Larochelle, Isabelle Lajoie, Yoshua Bengio, and Pierre-Antoine Manzagol. 2010. [Stacked denoising autoencoders: Learning useful representations in a deep network with a local denoising criterion](#). *J. Mach. Learn. Res.*, 11:3371–3408.
- Elena Voita, Rico Sennrich, and Ivan Titov. 2019. [The bottom-up evolution of representations in the transformer: A study with machine translation and language modeling objectives](#). In *Proceedings of the 2019 Conference on Empirical Methods in Natural Language Processing and the 9th International Joint Conference on Natural Language Processing (EMNLP-IJCNLP)*, pages 4396–4406, Hong Kong, China. Association for Computational Linguistics.
- Alex Wang, Amanpreet Singh, Julian Michael, Felix Hill, Omer Levy, and Samuel Bowman. 2018. [GLUE: A multi-task benchmark and analysis platform for natural language understanding](#). In *Proceedings of the 2018 EMNLP Workshop BlackboxNLP: Analyzing and Interpreting Neural Networks for NLP*, pages 353–355.
- Thomas Wolf, Lysandre Debut, Victor Sanh, et al. 2020. [Transformers: State-of-the-art natural language processing](#). In *Proceedings of the 2020 Conference on Empirical Methods in Natural Language Processing: System Demonstrations*, pages 38–45.
- Sangwon Yu, Jongyoon Song, Heeseung Kim, Seongmin Lee, Woo-Jong Ryu, and Sungroh Yoon. 2022. [Rare tokens degenerate all tokens: Improving neural text generation via adaptive gradient gating for rare token embeddings](#). In *Proceedings of the 60th Annual Meeting of the Association for Computational Linguistics (Volume 1: Long Papers)*, pages 29–45.
- Ying Zhang, Hidetaka Kamigaito, and Manabu Okumura. 2021. [A language model-based generative classifier for sentence-level discourse parsing](#). In *Proceedings of the 2021 Conference on Empirical Methods in Natural Language Processing*, pages 2432–2446, Online and Punta Cana, Dominican Republic. Association for Computational Linguistics.
- Zhong Zhang, Chongming Gao, Cong Xu, Rui Miao, Qinli Yang, and Junming Shao. 2020. [Revisiting representation degeneration problem in language modeling](#). In *Findings of the Association for Computational Linguistics: EMNLP 2020*, pages 518–527.

A Isotropy Metric and DelDirection

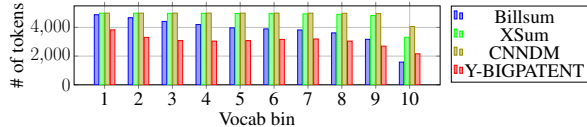
Isotropy Metric. \mathbf{E} denotes the pre-trained token embedding matrix of the PLM. Following previous studies (Mu et al., 2018; Biś et al., 2021; Yu et al., 2022), we compute the isotropy of \mathbf{E} using Eq.(1) from Mu et al. (2018), which is given by:

$$I(\mathbf{E}) = \frac{\min_{\mathbf{b} \in \mathcal{B}} Z(\mathbf{b})}{\max_{\mathbf{b} \in \mathcal{B}} Z(\mathbf{b})},$$

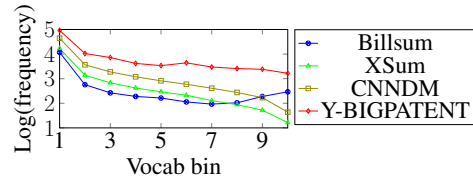
where $Z(\mathbf{b})$ is approximately constant, \mathcal{B} is the set of eigenvectors of $\mathbf{E}^T \mathbf{E}$ with T represents transposition operation.

DelDirection. We regard DelDirection as our baseline since it is also a post-processing technique and can be applied to token-level vocabularies to improve isotropy for \mathbf{E} . DelDirection eliminates the common mean vector and top- β dominating directions from \mathbf{E} . According to Mu et al. (2018), $\beta \approx h_e/100$, therefore we set $\beta = 10$.

B Downstream Datasets



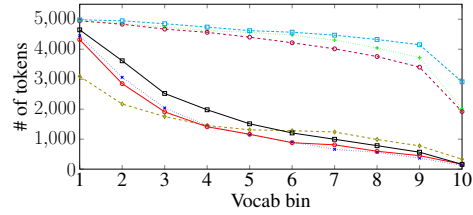
(a) Number of tokens appearing in vocabulary \mathcal{V} .



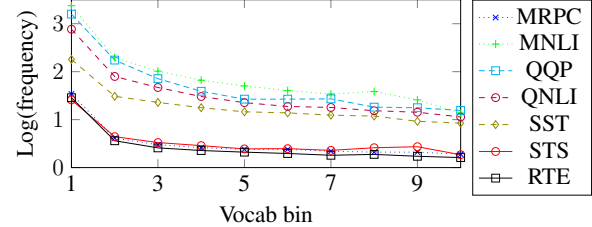
(b) Logarithmic averaged frequency of tokens appearing in the corresponding training set.

Figure 6: Distribution of the BART vocabulary \mathcal{V} in the training sets of text summarization datasets, considering both source and target tokens. The first 50,000 tokens in \mathcal{V} are grouped into bins of 5,000 according to their index in \mathcal{V} (e.g., [0:4,999]).

Dataset Description. Table 6 provides an overview of the data statistics for each task. For the GLUE task, we utilize Stanford Sentiment Treebank (SST), Microsoft Research Paraphrase Corpus (MRPC), Semantic Textual Similarity Benchmark (STS), Quora Question Pairs (QQP), MultiNLI (MNLI), Question NLI (QNLI), and Recognizing Textual Entailment (RTE) datasets. For the text summarization task, CNNDM (Hermann et al., 2015) comprises articles



(a) Number of tokens appearing in \mathcal{V} .



(b) Logarithmic averaged frequency of tokens appearing in the corresponding training set.

Figure 7: Distribution of the BART vocabulary in the training sets of GLUE datasets.

from CNN and Daily Mail newspapers, while Xsum (Narayan et al., 2018) consists of BBC articles paired with single-sentence summaries. BillSum (Kornilova and Eidelman, 2019) contains summaries of US Congressional and California state bills. Y-BIGPATENT is the “y” category of BIGPATENT (Sharma et al., 2019) and contains U.S. patent documents covering new or cross-sectional technology.

Dataset Distribution. Figures 6 and 7 show the distribution of tokens appearing in the GLUE and text summarization datasets. We observe that CNNDM dataset has the most uniform distribution and the greatest variety of appearing tokens among CNNDM, Y-BIGPATENT, XSum, and Billsum text summarization datasets. The token frequency in Y-BIGPATENT dataset is significantly higher than in the other datasets, despite having the smallest variety of appearing tokens. As these two figures show, the token frequency in text summarization datasets is much higher than that in the GLUE datasets. These findings suggest a potential difference when fine-tuning embeddings with respect to the task requirements.

Task	Dataset	# of train	# of validation	# of test
Word similarity	RG65 (Rubenstein and Goodenough, 1965)	-	-	65
	SimLex-999 (Hill et al., 2015)	-	-	999
	RW (Luong et al., 2013)	-	-	2,034
	SimVerb-3500 (Gerz et al., 2016)	-	-	3,500
GLUE	RTE	2,490	277	3,000
	MRPC	3,668	408	1,725
	STS	5,749	1,500	1,379
	SST	67,349	872	1,821
	QNLI	104,743	5,463	5,463
	QQP	363,846	40,430	390,965
	MNLI	392,702	9,815 (m) + 9,832 (mm)	9,796 (m) + 9,847 (mm)
Text summarization	BillSum	17,054	1,895	3,269
	Y-BIGPATEMENT	124,397	6,911	6,911
	XSum	204,045	11,332	11,334
	CNNNDM	287,227	13,368	11,490

Table 6: Detailed statistic of train, validation and test datasets. For the MNLI dataset, we report Matched (m) and Mismatched (mm) sets.

C Geometric Distribution of Embeddings

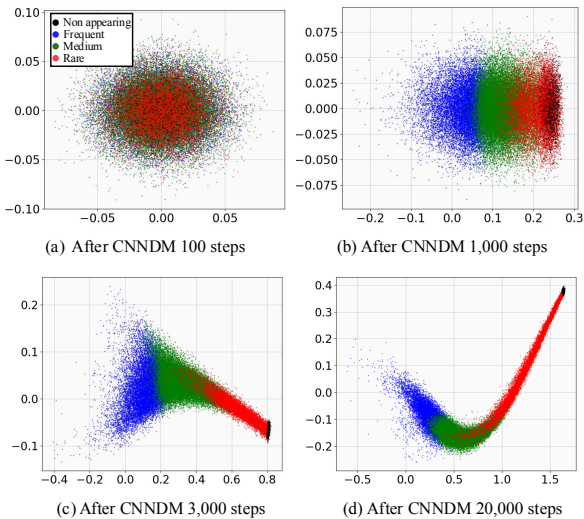


Figure 8: Projected token embeddings of a randomly initialized model (BART architecture) training on the CNNNDM dataset. 30%, 50%, and 20% of the appearing tokens in BART’s vocabulary \mathcal{V} are assigned to the frequent, medium, and rare groups, respectively, based on their frequency in the training set.

Fragile Embeddings without Pre-training. To investigate whether pre-training helps models to be robust against degeneration into a cone shape, we compare pre-trained BART with a randomly initialized model (BART architecture). As shown in Figure 8, after 1,000 training steps, the initialized model exhibits obvious degeneration, and after 3,000 steps, the shape of its embeddings becomes more like a narrow cone. This result aligns well with previous studies (Gao et al., 2019; Yu et al., 2022). In contrast, the pre-trained BART

does not show such degeneration (Figure 2).

Degeneration with More Updating. Figures 9 (e) and (g) show that before fine-tuning, the embeddings of DelDirection form a narrow ellipse. After fine-tuning, the minor axis of the ellipse lengthens, and the frequent, medium, and rare groups gradually disperse, eventually forming a square, as shown in Figures 9 (f) and (h). From Figures 9 (f) and (h), we also observe that the more updating steps, the longer the original minor axis of the ellipse, and the higher $I(\mathbf{E})$ achieves by DelDirection. However, if DelDirection is fine-tuned further, the shape may resemble that in Figure 2 (h), resulting in a much smaller $I(\mathbf{E})$. Comparing Figures 9 (a) to (d) with Figures 9 (i) to (l), we observe that BART + DefinitionEMB performs similarly to BART. Specifically, on the XSum dataset, there is minimal drift in embeddings from “before” to “after” fine-tuning. Conversely, for the Billsum dataset, after fine-tuning, the embeddings of two ellipses move closer together.

Architecture-Irrelevant Robustness. We do not observe drift for BART-related models on the QQP and RTE datasets, as shown in Figure 10, which is different from text summarization datasets. This may be because the BART for classification tasks does not use the weight tying technique, and the token frequencies in QQP and RTE are much lower than in text summarization datasets. Using DelDefinition for RoBERTa shows the spread of popular tokens from the original center, as shown in Figures 11 (e) and (f). Although RoBERTa and BART have different model architectures

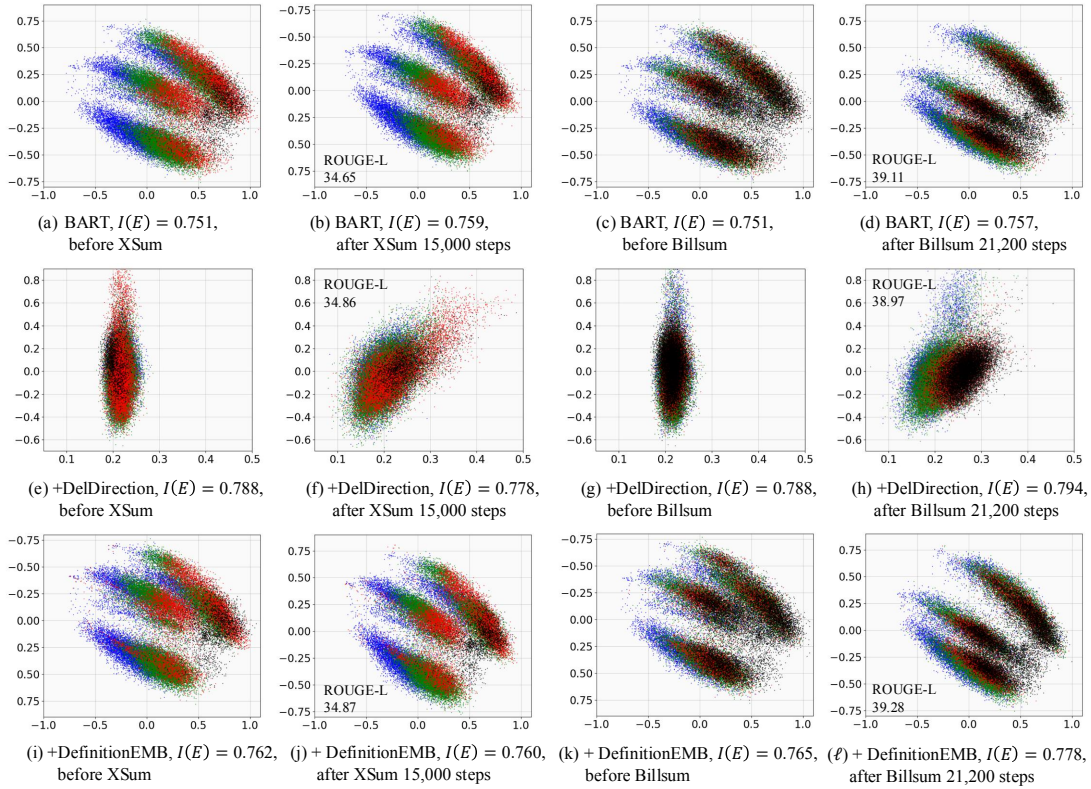


Figure 9: Projected token embeddings of BART-related models before to after fine-tuning on the XSum and Billsum datasets. 30%, 50%, and 20% of tokens appearing in \mathcal{V} are assigned to the frequent, medium, and rare groups, respectively, based on their frequency in the fine-tuning set.

(encoder-only vs. encoder-decoder), scales, and pre-training strategies, they both show similar robustness against representation degeneration. This suggests that PLMs’ robustness against representation degeneration might not be directly related to these variables.

Case Studies. Figures 12, 13, and 14 show case studies of specific tokens before and after replacing their token embeddings. Non-appearing, rare, medium, and frequent groups in the CNNDM dataset are represented by black, red, green, and blue points respectively. In BART, the central tokens are surrounded by tokens of the same frequency, rather than those with related semantics. In the case of BART+DelDirection, we observe tokens with different token frequencies surrounding the central word. However, using DelDirection also does not guarantee semantically related neighbors. After replacing embeddings with DefinitionEMB, semantically related tokens appear in the surrounding of the central tokens.

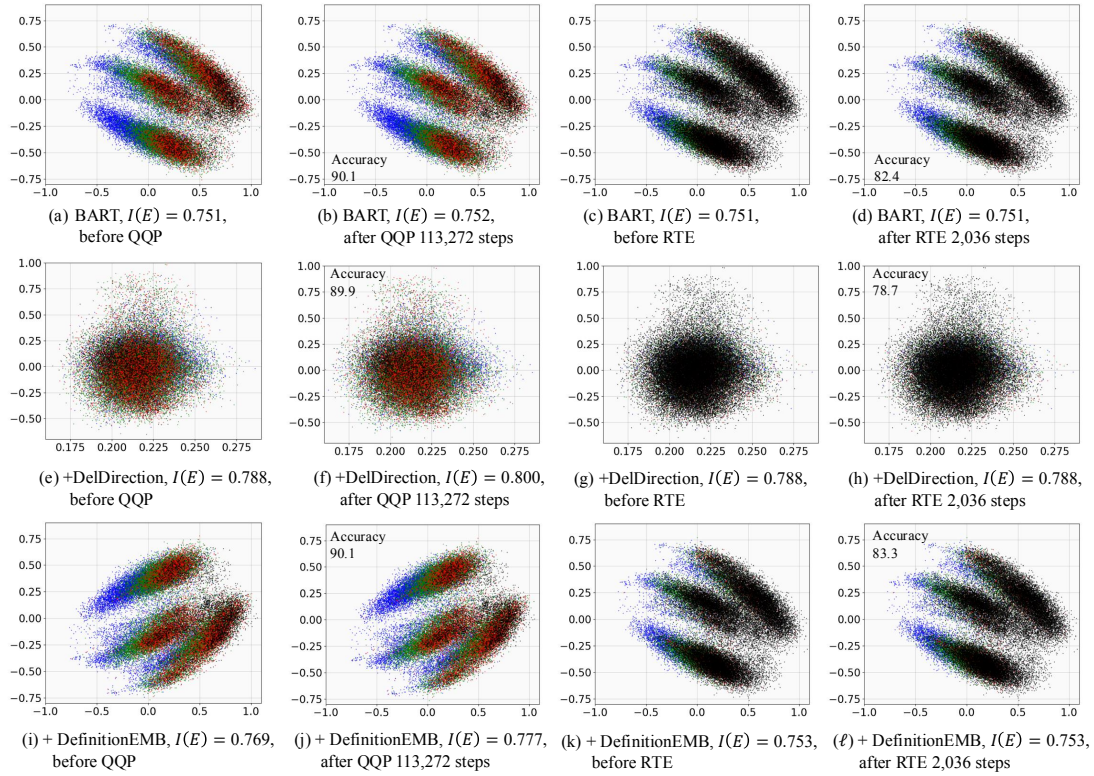


Figure 10: Projected token embeddings of BART-related models “before” and “after” fine-tuning on the QQP and RTE datasets.

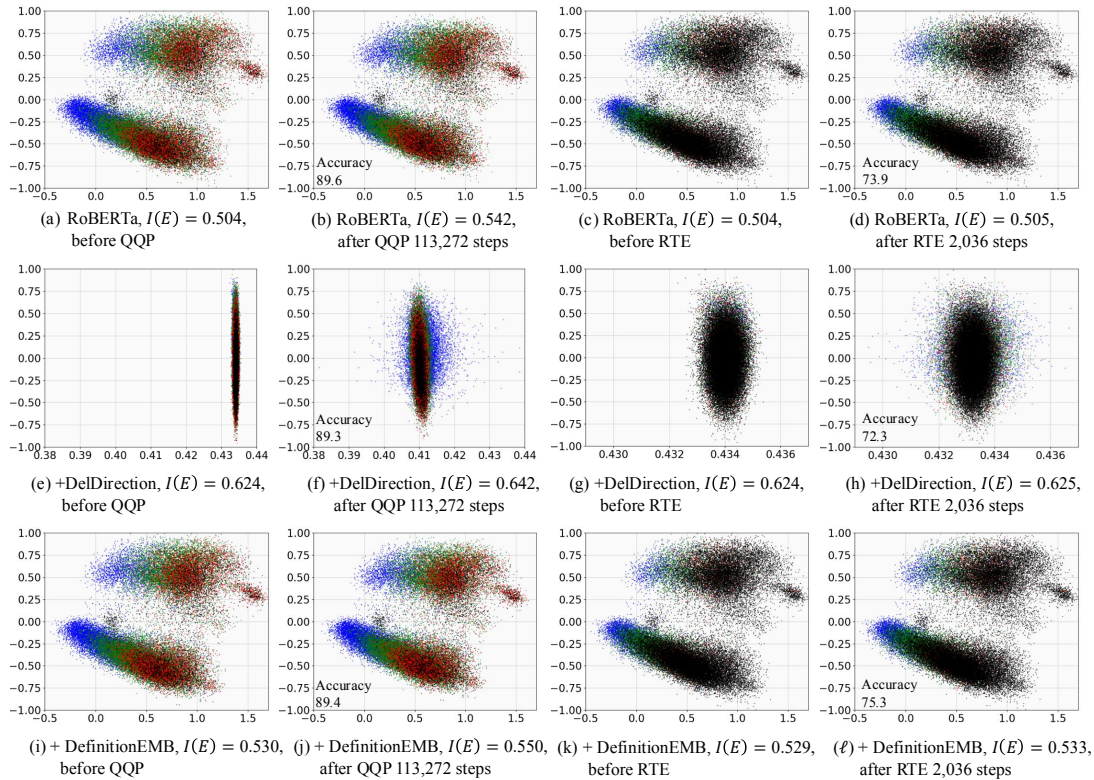


Figure 11: Projected token embeddings of RoBERTa-related models “before” and “after” fine-tuning on the QQP and RTE datasets.

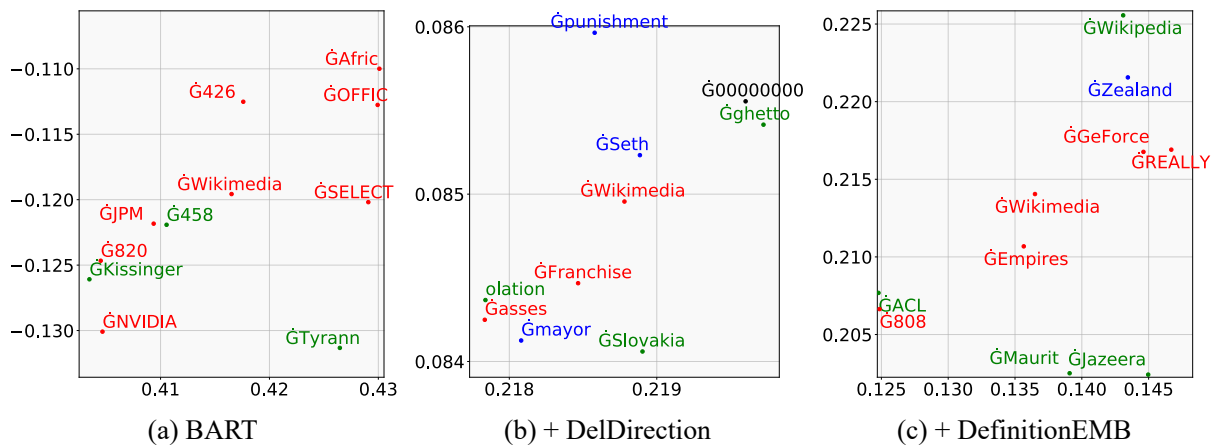


Figure 12: Case study of the token embeddings of the token "GWikimedia" and its surrounding tokens, where "G" denotes whitespace.

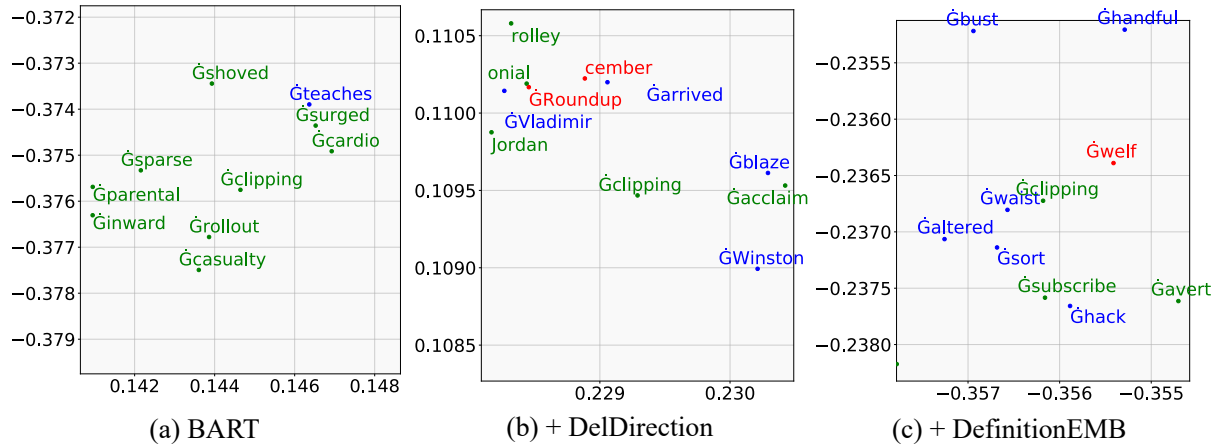


Figure 13: Case study of the token embeddings of the token "Gclipping" and its surrounding tokens.

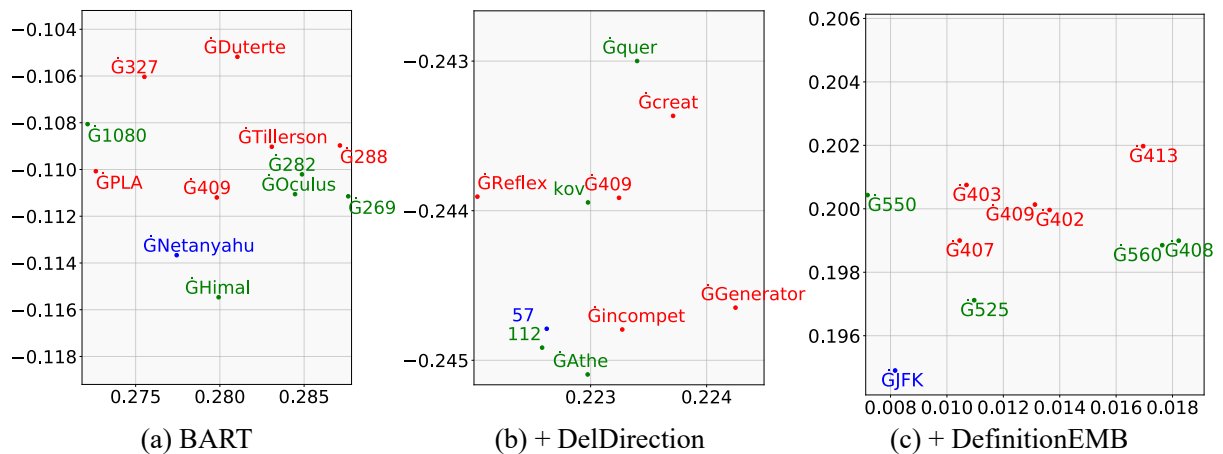


Figure 14: Case study of the token embeddings of the token "G409" and its surrounding tokens.

Query	Please help me to check the semantic relationship between the token “everlasting” and other tokens, including reassure, legalize, validate, underworld, typo, misdemeanor, jurisd, scripting, APIs, io, bye, complaining, LAB, arcade, incentive, hematically, mind, stagn, sun, vast, star, tw, general, click, rusty. Please return scores in the range [0,1] to indicate their semantic relationship, and tell me the reason.
ChatGPT 3.5	<p>validate: 0.3 - "Validate" can mean to confirm or verify the accuracy or truth of something, which could have a moderate semantic relationship with "everlasting" if used in a context related to eternal validity or truth.</p> <p>mind: 0.2 - "Mind" refers to the faculty of consciousness and thought, which could have a moderate semantic relationship with "everlasting" if used in a context related to eternal consciousness or existence.</p> <p>sun: 0.3 - "Sun" refers to the star around which the Earth orbits and has a moderate semantic relationship with "everlasting" due to its association with eternal cycles and longevity.</p> <p>vast: 0.3 - "Vast" refers to something extremely large or extensive, which could have a moderate semantic relationship with "everlasting" if used in a context related to eternal expansiveness.</p> <p>star: 0.3 - "Star" refers to a celestial body that emits light and has a moderate semantic relationship with "everlasting" due to its association with eternal cycles and longevity.</p>
Claude 3 Haiku	<p>"everlasting" and "validate": Score: 0.4 Reason: "Everlasting" and "validate" share a sense of permanence and confirmation, as "validate" means to confirm or corroborate something as true or correct, which is somewhat related to the idea of something being eternal or lasting forever.</p> <p>"everlasting" and "mind": Score: 0.4 Reason: "Everlasting" suggests something that lasts forever, while the "mind" is a key part of human consciousness and experience, which are somewhat related in the sense that the human mind may be seen as an eternal or enduring aspect of the self.</p> <p>"everlasting" and "sun": Score: 0.4 Reason: "Everlasting" suggests something that lasts forever, and the "sun" is a celestial body that has existed for billions of years and is expected to continue shining for a very long time, so there is a connection between the idea of something being "everlasting" and the sun's enduring presence.</p> <p>"everlasting" and "vast": Score: 0.5 Reason: "Everlasting" suggests something that is immense or boundless in its duration, while "vast" describes something that is immense in size or scope, so there is a semantic overlap between the two terms in terms of conveying a sense of immensity or grandeur.</p> <p>"everlasting" and "star": Score: 0.4 Reason: Similar to the connection with the "sun", the "star" is another celestial body that exists for long durations, so the idea of something being "everlasting" is somewhat related to the enduring nature of stars.</p>

Table 7: The query to ChatGPT 3.5 and Claude 3 Haiku, along with part of their responses.

(a) Full prompt

The _ definition _ of _ discomfort _ is _ To _ cause _ annoyance _ or _ distress _ to _ . _ Its _ part-of-speech _ , _ bpe-form _ without _ space _ , _ capitalization _ , _ and _ uppercase _ are _ verb _ , _ discomfort _ , _ Discomfort _ , _ and _ DISCOMFORT _ , _ respectively _ .

(b) Source for the encoder-decoder PLM

The _ definition _ of <MASK₁> _ is _ To _ cause _ annoyance _ or _ distress _ to _ . _ Its _ part-of-speech _ , _ bpe-form _ without _ space _ , _ capitalization _ , _ and _ uppercase _ are _ verb _ , _ <MASK₂> _ , _ <MASK₃> _ , _ and _ <MASK₄> _ , _ respectively _ .

(c) Target for the encoder-decoder PLM

<MASK₁> _ discomfort <MASK₂> discomfort <MASK₃> _ Discomfort <MASK₄> _ DISCOMFORT

(d) Source for the encoder-only PLM during training

The _ definition _ of <MASK> _ is _ To _ cause _ annoyance _ or _ distress _ to _ . _ Its _ part-of-speech _ , _ bpe-form _ without _ space _ , _ capitalization _ , _ and _ uppercase _ are _ verb _ , _ <MASK>comfort _ , _ GDis <MASK> _ , _ and <MASK> COM *BS GNations* _ , _ respectively _ .

(e) Source for the encoder-only PLM during inference

The _ definition _ of <MASK> _ is _ To _ cause _ annoyance _ or _ distress _ to _ . _ Its _ part-of-speech _ , _ bpe-form _ without _ space _ , _ capitalization _ , _ and _ uppercase _ are _ verb _ , _ discomfort _ , _ Discomfort _ , _ and _ DISCOMFORT _ , _ respectively _ .

Figure 15: Example of constructing prompts for the word “discomfort”. “_” is whitespace. <MASK_i> denotes the ith mask token. *Italic* indicates randomly replaced tokens.

D Semantically Related Tokens Recognized by Large Language Models

Table 7 shows the query we used to ask ChatGPT 3.5 and Claude 3 Haiku about the semantic relationship between “Geverlasting” and other tokens, along with their corresponding responses for semantics-related tokens only.

E Settings for DefinitionEMB

E.1 Details of Cloze Exercise

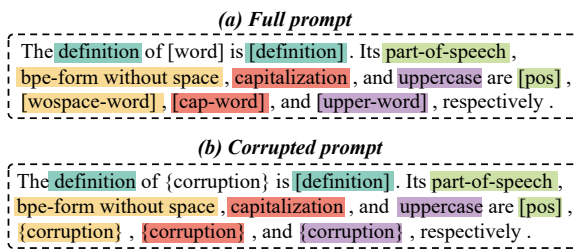


Figure 16: Constructed prompts. Brackets [] are a placeholder for the given word and its corresponding information. Texts with the same color indicate positions of a prompt and corresponding word information. {corruption} indicates the span for corrupted tokens. The bpe-form without space refers to the word’s surface-form without the symbol “Ġ” when using the BART’s tokenizer.

Full Prompt. As shown in Figure 16 (a), to include complete definition for better re-construction, our full prompt incorporates the definition, part-of-speech, capitalization, and case sensitivity of the word w , along with the tokenizer’s specific settings. Figure 15 (a) shows examples of full prompt for the word “discomfort”.

Corruption Strategy. As shown in Figures 16 (b), parts of tokens within the corruption spans are randomly corrupted, as detailed below.

For encoder-only PLM, as shown in Figures 15 (d-e), tokens within the corruption spans are corrupted using a BERT-style masking strategy. Specifically, during training, 50% of the tokens are replaced with a special mask token <MASK>, 25% are replaced with a random token, and the remaining 25% are left unchanged.⁷ During inference, only one token within the corruption spans is

replaced with <MASK> at a time, and this procedure is repeated until all tokens in the corruption spans have been replaced.

For the encoder-decoder PLM, as shown in Figures 15 (b-c), we follow the T5-style masking approach by Raffel et al. (2020) to corrupt tokens. Specifically, we replace each corruption span with a mask token to construct the source sequence. Subsequently, we construct the target sequence using the replaced tokens delimited by the mask tokens used for replacement.

Embedding Reconstruction. DefinitionEMB re-constructs embedding as follows:

For the encoder-only model, we re-construct embedding according to the masked language modeling (Devlin et al., 2019). Let v_k be a corrupted token, with $k \in \kappa$ indicating its position in the full prompt. We utilize the corrupted prompt as input, where v_k is replaced by <MASK>. And then, the last hidden states s_k is computed at position k and mapped to the re-constructed embedding of v_k .

For the encoder-decoder model, we re-construct embedding according to the causal language modeling (Hyndman and Athanasopoulos, 2018). The constructed target sequence is denoted as $\mathbf{y} = (y_1, \dots, y_{2J})$, where J is the number of corrupted tokens. For any $j \in [1, J]$, y_{2j} and y_{2j-1} denote corrupted tokens and their corresponding delimiters, respectively. Input the source and prefix target tokens $\mathbf{y}_{<2j} = (y_1, \dots, y_{2j-1})$, we map the last hidden states of y_{2j-1} to the re-constructed embedding of y_{2j} in the decoder.

⁷Our pre-experiments demonstrate that a large mask ratio would result in slow convergence, while a small ratio would cause limited change between $\mathbf{e}(v)$ and $\tilde{\mathbf{e}}(v)$. To ensure computational efficiency and to prevent the model from relying too heavily on unmasked tokens, we manually set these ratios.

E.2 Pre-experiment for Replacing Strategy

Strategy	RoBERTa	BART
None	87.5	87.8
Random	87.4	87.3
Top	86.0	87.6
Last	87.7	88.3

Table 8: Using three different strategies to replace tokens in \mathcal{V}_{MRPC} with DefinitionEMB ($\alpha = 5$) for RoBERTa-base and BART-large on the MRPC test set.

Considering the appearance bias as indicated in Figures 2 (e) and (j), we conduct pre-experiments to investigate which type of tokens in $\mathcal{V}_{[task]}$ should be replaced. DefinitionEMB replaced the embeddings of $\min(\alpha\% * |\mathcal{V}|, |\mathcal{V}_{[task]}|)$ of tokens in $\mathcal{V}_{[task]}$ using one of the following strategies:

Random: Randomly replace tokens.

Top: Replace top tokens in $\mathcal{V}_{[task]}$, where index ≥ 5000 .

Last: Replace last tokens in $\mathcal{V}_{[task]}$.

As shown in Table 8, replacing the last tokens in $\mathcal{V}_{[task]}$ results in the highest accuracy.

F Hyperparameters

Hyperparameters	RoBERTa	BART
# of updates	400,000	250,000
# of warm-up updates	24,000	20,000

Table 9: Hyperparameters used for training DefinitionEMB initialized from BART and RoBERTa.

Hyperparameters	SST	MRPC	STS	QQP	MNLI	QNLI	RTE
# of updates	20,935	2,296	3,598	113,272	123,873	33,112	2,036
# of warm-up updates	1,256	137	214	28,318	7,432	1,986	122
Batch size (sentences)	32	16	16	32	32	32	16
Learning rate	1e-5	1e-5	2e-5	1e-5	1e-05	1e-05	2e-05

Table 10: Hyperparameters used for fine-tuning RoBERTa-related models across different datasets.

Used Artifacts. Table 11 lists the artifacts utilized in the study. We use the Fairseq (Ott et al., 2019) and HuggingFace (Wolf et al., 2020) to reproduce all models and run the downstream tasks.

We adhere to the original fine-tuning settings of RoBERTa and BART on the GLUE task and CNNDM dataset. BART utilizes the weight

tying (Press and Wolf, 2017) technique when predicting texts, which involves using \mathbf{E} as the weight matrix for computing logits. Details of the hyperparameter settings for training DefinitionEMB and fine-tuning models are outlined in Tables 9, 10, and 12. During the training of DefinitionEMB, we utilize the Adam optimizer with a batch size of 4,096 tokens and a 0.0001 learning rate with an “inverse square root” schedule. For fine-tuning models on GLUE and text summarization tasks, we employ the Adam optimizer and utilized a “polynomial decay” learning rate schedule. To reduce computation, we freeze the embedding layer of DefinitionEMB during training for BART. As for the initialized model in Figure 8, we set learning rate, batch size (tokens), number of updates, and number of warm-up steps as 0.001, 64,000, 50,000, and 4,000, respectively.

Definitions for Numbers and Named Entities. We add definitions for 1,252 numbers in PLM’s vocabulary \mathcal{V} by translating numbers into their corresponding words, such as “2” to “two”. Furthermore, we added definitions for 136 named entity tokens in \mathcal{V} , such as “NVIDIA”, based on their Wikipedia pages or Google search results. These definitions are available at our anonymous Github <https://anonymous.4open.science/r/DefinitionEMB-2754>.

Rare Token Subset. To construct the rare token subset that used in Table 5, we first filter the CNNDM test set to include target sentences whose tokens all appear in the training set. Additionally, each filtered target sentence must contain at least 5% rare tokens with indices larger than 40,000 in \mathcal{V} , and these tokens’ embeddings can be replaced by DefinitionEMB. This process finally yield 65 pairs of data. This subset is also available at our anonymous Github.

Tuning α . For each downstream task, we tune α with a single trial on the corresponding validation set. Tables 13 to 23 display the performance of Baseline+DefinitionEMB with various α . Tables 24 and 25 provide the tuned α for each downstream dataset. Overall, datasets in the GLUE task exhibit smaller α than those in the text summarization task. This may be because the text summarization task involves a larger number of input tokens than the GLUE task. Additionally, the text summarization task involves predicting tokens,

Used artifacts	Note
RoBERTa	https://huggingface.co/roberta-base
BART	https://huggingface.co/facebook/bart-large
BART for GLUE	https://github.com/facebookresearch/fairseq/blob/main/examples/bart/README.glue.md
BART for CNNDM	https://github.com/facebookresearch/fairseq/blob/main/examples/bart/README.summarization.md
Wiktionary	https://en.wiktionary.org/wiki/Wiktionary:Main_Page
Wiktionary(extracted)	https://github.com/tatuylonen/wiktextextract/tree/master
Isotropy metric	https://github.com/danielbis/tooMuchInCommon/blob/main/src/isotropy.py
View contextual embedding	https://github.com/TideDancer/iclr21_isotropy_contxt
Files2rouge	https://github.com/pltrdy/files2rouge
Paired bootstrap resampling	https://github.com/neubig/util-scripts/blob/master/paired-bootstrap.py
Fairseq	https://github.com/facebookresearch/fairseq/
HuggingFace	https://github.com/huggingface/transformers/
ChatGPT 3.5	https://chat.openai.com/
Claude 3 Haiku	https://claude.ai/chat/

Table 11: Used artifacts.

Hyperparameters	SST	MRPC	STS	QQP	MNLI	QNLI	RTE	CNNDM	Y-BIGPATENT	XSUM	Billsum
# of updates	7,150	700	1,800	113,920	43,210	33,290	1020	20,000	92,880	15,000	21,320
# of warm-up updates	429	42	108	6,835	2,593	1,997	61	500	7,430	500	1,705
Batch size (sentences)	128	64	32	32	256	32	32	-	-	-	-
Batch size (tokens)	-	-	-	-	-	-	-	65,536	8,192	32,768	8,192
Learning rate	5e-6	2e-5	2e-5	1e-5	5e-6	1e-5	1e-5	3e-05	3e-5	3e-05	3e-5

Table 12: Hyperparameters used for fine-tuning BART-related models across different datasets.

whereas BART employs a weight tying technique to connect token embeddings for prediction, enabling token embeddings to be updated more during fine-tuning than in the GLUE task. Among all datasets, the SST dataset has the smallest tuned α , set at 1. This could be attributed to the dataset having the fewest unique tokens. The STS, RTE, and MRPC datasets have a similar number of unique tokens, slightly higher than that of the SST dataset, resulting in α values of 3 and 5. In the GLUE task, the QQP, QNLI, and MNLI datasets have the highest number of unique tokens, leading to α values for BART of 3, 5, and 10, respectively. However, tuned α values of the three datasets for RoBERTa are all set to 3: this may be because MSE is larger in RoBERTa than in BART as discussed in Appendix G.2. Among the text summarization datasets, Billsum has the lowest token frequencies, resulting in the smallest α value of 7. Despite having the highest token frequencies, the Y-BIGPATENT dataset has the lowest number of unique tokens, resulting in an α value of only 30. The CNNDM dataset yields the highest α value, set at 100, possibly due to its most uniformly distributed and largest number of unique tokens, and larger training corpus. Although the XSum dataset also contains a large number of unique tokens, it has a smaller training corpus

than CNNDM, resulting in a smaller α value of 10. These findings suggest a potential relationship between the distribution of training data and the value of α . Specifically, datasets with a larger number of unique tokens, along with more training examples, tend to result in higher α values.

Baseline \ α	1	5	10	20
RoBERTa	89.2	90.2	89.5	89.7
BART	88.2	90.2	88.7	89.2

Table 13: Accuracy for Baseline+DefinitionEMB with various α on the MRPC validation set.

Baseline \ α	1	5	10	20
RoBERTa	95.1	94.8	94.8	94.4
BART	96.2	96.1	95.6	95.3

Table 14: Accuracy for Baseline+DefinitionEMB with various α on the SST validation set.

Baseline \ α	3	5	10	20
RoBERTa	77.3	79.1	76.2	76.5
BART	85.9	85.9	84.8	84.1

Table 15: Accuracy for Baseline+DefinitionEMB with various α on the RTE validation set.

Baseline \ α	3	5	7	10
RoBERTa	90.7	90.5	90.3	90.3
BART	91.8	91.7	91.5	91.3

Table 16: Spearman’s rank correlation for Baseline+DefinitionEMB with various α on the STS validation set.

Baseline \ α	3	7	10	30
RoBERTa	92.9	92.9	92.8	92.5
BART	94.8	94.7	94.5	94.4

Table 17: Accuracy for Baseline+DefinitionEMB with various α on the QNLI validation set.

Baseline \ α	3	5	10	30
RoBERTa	91.8	91.7	91.8	91.8
BART	92.4	92.6	92.5	92.2

Table 18: Accuracy for Baseline+DefinitionEMB with various α on the QQP validation set.

Baseline \ α	3	5	10	30
RoBERTa	87.6	87.5	87.4	87.3
BART	89.7	89.6	89.8	89.6

Table 19: Accuracy for Baseline+DefinitionEMB with various α on the MNLI validation set.

α	ROUGE (F1)		
	1	2	L
10	44.45	21.62	41.17
30	44.30	21.44	41.04
50	44.23	21.37	40.99
100	44.62	21.54	41.40

Table 20: ROUGE scores for BART+DefinitionEMB with various α on the CNNDM validation set.

α	ROUGE (F1)		
	1	2	L
5	44.02	20.66	34.95
10	44.22	20.95	35.24
20	43.81	20.55	34.78
100	42.46	19.18	33.62

Table 21: ROUGE scores for BART+DefinitionEMB with various α on the XSUM validation set.

α	ROUGE (F1)		
	1	2	L
5	50.63	32.19	38.81
7	50.85	32.44	39.10
10	51.08	32.17	38.97
100	50.04	31.43	38.27

Table 22: ROUGE scores for BART+DefinitionEMB with various α on the Billsum validation set.

α	ROUGE (F1)		
	1	2	L
10	43.62	18.53	37.43
20	43.93	18.84	37.74
30	44.22	19.12	38.03
100	42.96	17.76	36.73

Table 23: ROUGE scores for BART+DefinitionEMB with various α on the Y-BIGPATENT validation set.

Model	MRPC	SST	RTE	STS	QNLI	QQP	MNLI
RoBERTa	5	1	5	3	3	3	3
BART	5	1	3	3	3	5	10

Table 24: Tuned α for GLUE datasets.

Model	CNNDM	Y-BIGPATENT	XSUM	Billsum
BART	100	30	10	7

Table 25: Tuned α for text summarization datasets.

G Additional Evaluation

G.1 Projected Initial Token Embeddings

Figure 17 shows the projected token embeddings of models before and after replacing E completely.

G.2 Differences in DefinitionEMB with Regard to Model Architecture

Token	Index in \mathcal{V}	MSE
sys	43103	23.3829
ĠNASL	47179	23.2779
resso	27989	23.2549
ĠFAQ	39313	22.8146
ĠpH	39228	22.1278
ĠB	163	0.0061
ER	2076	0.0059
s	29	0.0055
ING	1862	0.0051
-	12	0.0040

Table 26: Top and bottom 5 tokens based on the degree of MSE estimated by DefinitionEMB based on RoBERTa model, listed in descending order of MSE.

Token	Index in \mathcal{V}	MSE
ourke	18338	18.7777
esson	24711	17.6324
aeus	39174	17.3797
wagen	42099	16.8839
auga	24491	16.8624
ER	2076	0.0020
ES	1723	0.0020
ING	1862	0.0020
-	12	0.0018
S	104	0.0018

Table 27: Top and bottom five tokens based on the degree of MSE estimated by DefinitionEMB based on BART model, listed in descending order of MSE.

Different MSE Distributions. For tokens in PLM’s vocabulary \mathcal{V} , we analyze the mean squared error (MSE) between their pre-trained and definition embeddings. Figure 18 presents the results for DefinitionEMB on the RoBERTa model. The left subfigure illustrates that around 20% of the tokens have an MSE of less than

1, while less than 20% tokens have an MSE larger than 8. The right subfigure shows that the distribution of token index is almost uniform across the MSE, indicating that the pre-trained embedding of high-frequency tokens may contain semantically unrelated information, while the pre-trained embedding of low-frequency tokens may contain semantically related information even with limited pre-training steps. In addition, more tokens fall in the MSE range of [5, 8) than in the range of [0, 1), which indicates a significant difference between pre-trained embeddings and definition embeddings. Figure 19 presents the results for DefinitionEMB on the BART model. The left subfigure illustrates that around 40% of the tokens have an MSE of less than 1, while less than 10% tokens have an MSE larger than 8. The right subfigure also shows that the distribution of token index is almost uniform across the MSE. However, most of the tokens fall in the MSE range [0, 1), indicating less difference between pre-trained embeddings and definition embeddings than in the case of RoBERTa. Tables 26 and 27 list examples of tokens with the corresponding MSE. The top five tokens with the highest MSE can be used as named entities.

Reasons. The MSE results align with the original representation distribution in PLMs, where RoBERTa has fewer embedding parameters and exhibits lower isotropy than BART (Table 1). Because DefinitionEMB considers the pre-trained embeddings as gold embeddings, its constructed embeddings for RoBERTa naturally exhibit lower isotropy and higher MSE than those for BART. Additionally, the different masking strategies for encoder-only and encoder-decoder architectures may also lead to the different MSE and isotropy distributions, as Raffel et al. (2020) demonstrate that the T5-style masking mechanism is more effective than the BERT-style masking for the encoder-decoder model during pre-training.

G.3 Word Similarity Task Using Cosine Similarity

Table 28 shows the results for word similarity tasks, where the similarity between word embeddings is calculated using cosine similarity. Comparing Table 28 with Table 2, we observe that when using the dot product, DefinitionEMB achieves a higher Spearman score than BART. However, when using cosine similarity, the opposite result is observed.

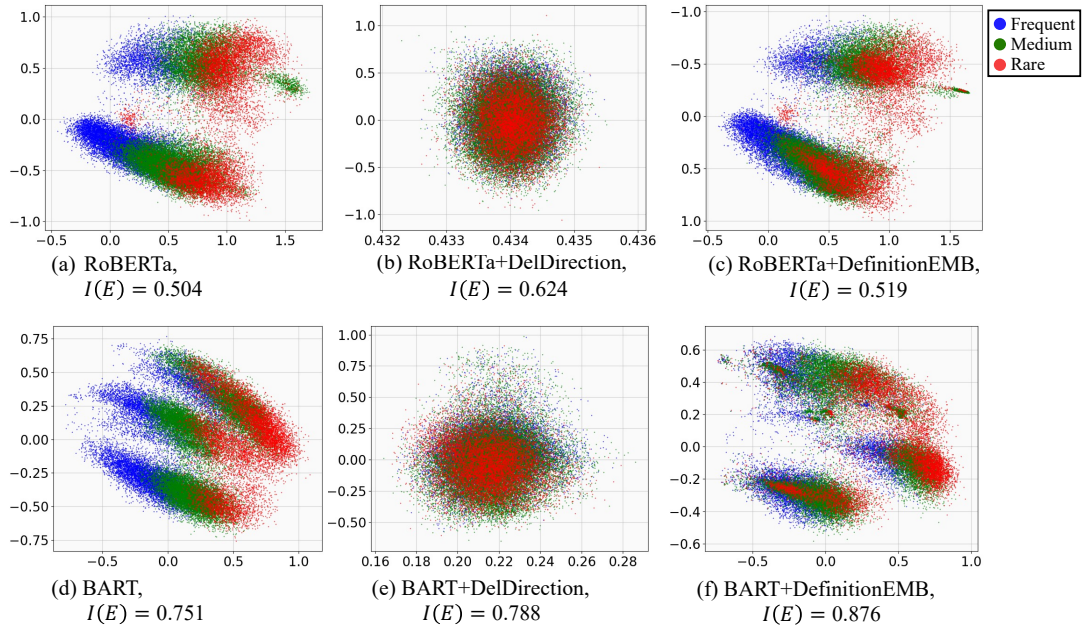


Figure 17: Projected token embeddings of models before and after replacing \mathbf{E} completely. The frequent (30%), medium (50%), and rare (20%) groups are determined based on the token index in \mathcal{V} .

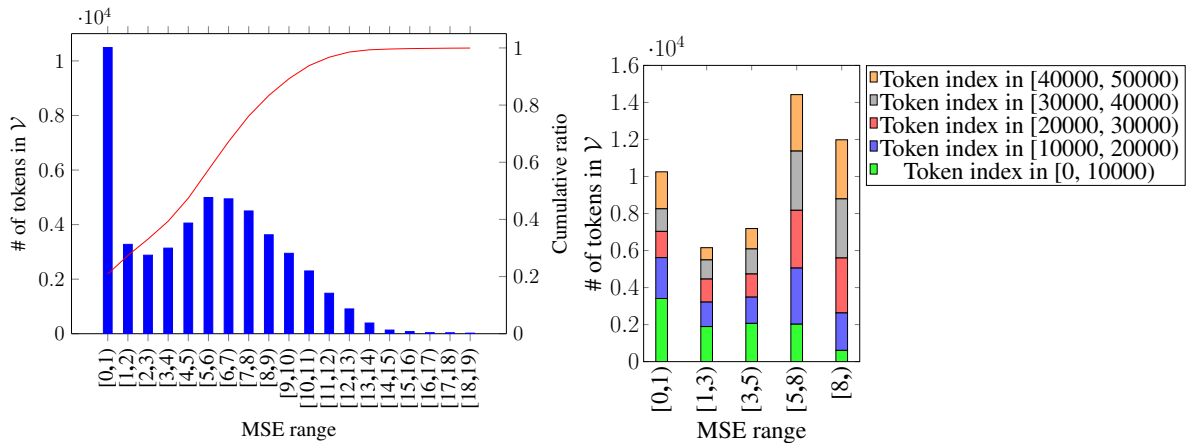


Figure 18: Number of tokens in \mathcal{V} versus MSE estimated by DefinitionEMB based on RoBERTA model.

Model	Spearman Score \uparrow				Ave
	RG65	RW	SimLex	SimVerb	
RoBERTa	25.55	22.33	18.04	10.78	19.18
+ DefinitionEMB	29.56	22.82	17.48	10.58	20.11
BART	24.35	23.20	22.00	12.73	20.57
+ DefinitionEMB	22.93	23.40	21.04	12.09	19.87

Table 28: Experimental results on the word similarity task with cosine similarity. DefinitionEMB replaces \mathbf{E} completely.

It indicates that the constructed embeddings for BART prioritize distance over angle aspects from the pre-trained embeddings.

G.4 Isotropy on GLUE Task

Table 29 presents $I(\mathbf{E})$ for models before and after fine-tuning on the GLUE task. Because $I(\mathbf{E})$ of PLMs and the DelDirection model before fine-tuning does not depend on $\mathcal{V}_{[task]}$, it is reported only once in the table. For the MRPC, STS, and RTE datasets, $I(\mathbf{E})$ shows a minimal difference between before and after fine-tuning models, likely due to the limited number of fine-tuning steps on these datasets. The token embedding distribution in BART appears to be more stable than RoBERTa on the SST, QQP, and MNLI datasets. Using DelDirection for RoBERTa and BART achieves the highest $I(\mathbf{E})$ across all datasets; however, it also results in the lowest accuracy and Pearson/Spearman’s rank

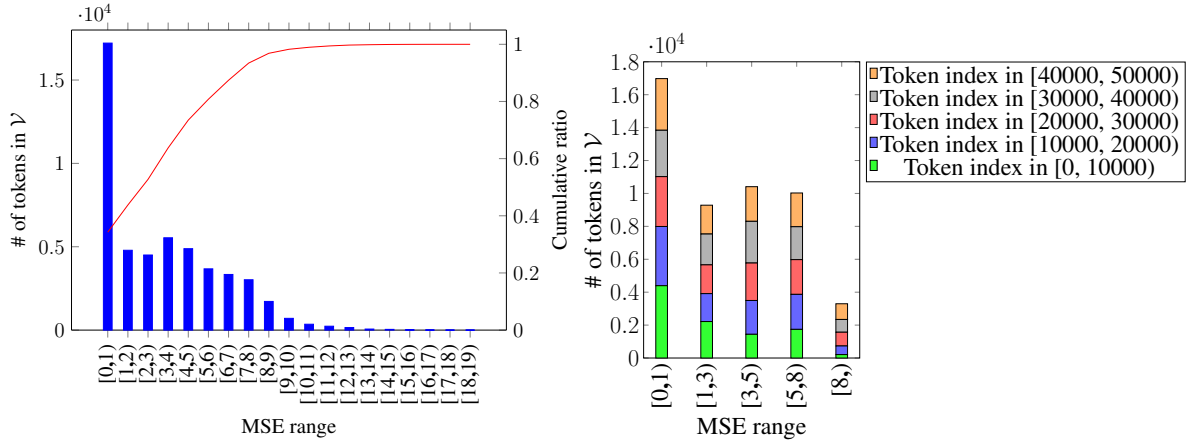


Figure 19: Number of tokens in \mathcal{V} versus MSE estimated by DefinitionEMB based on BART model.

Model	SST		MRPC		STS		QQP		MNLI		QNLI		RTE	
	Before	After	Before	After	Before	After	Before	After	Before	After	Before	After	Before	After
RoBERTa	0.504	0.533	-	0.505	-	0.506	-	0.542	-	0.544	-	0.509	-	0.505
+DelDirection	0.624	0.627	-	0.624	-	0.625	-	0.642	-	0.639	-	0.629	-	0.625
+DefinitionEMB	0.528	0.536	0.529	0.529	0.529	0.530	0.530	0.550	0.530	0.554	0.539	0.541	0.529	0.533
BART	0.751	0.751	-	0.751	-	0.751	-	0.752	-	0.751	-	0.751	-	0.751
+DelDirection	0.788	0.788	-	0.788	-	0.788	-	0.800	-	0.805	-	0.794	-	0.788
+DefinitionEMB	0.766	0.766	0.767	0.767	0.769	0.769	0.769	0.777	0.770	0.771	0.753	0.753	0.753	0.753

Table 29: $I(\mathbf{E})$ for models before and after fine-tuning on the GLUE task.

correlation in most cases, as shown in Table 3. This supports our assumption that DelDirection model focuses on the distribution of embeddings at the expense of semantic information.

G.5 Ablation Study for Replacing Tokens

Replaced tokens	Y-BIGPATENT ($X = 23,000$)	Billsum ($X = 41,000$)
Appearing	44.16 / 19.06 / 38.01	50.96 / 32.64 / 39.28
Both	44.00 / 18.90 / 37.84	51.23 / 32.44 / 39.20

Table 30: Replacing appearing tokens only vs. replacing both appearing and non-appearing tokens for BART on the Y-BIGPATENT and Billsum test sets.

Model	Replaced tokens	MRPC
RoBERTa	Appearing	87.7
	Both	87.3
BART	Appearing	88.3
	Both	88.1

Table 31: Replacing appearing tokens only vs. replacing both appearing and non-appearing tokens for RoBERTa and BART on the MRPC test set with $X = 24,900$.

We conducted an ablation study to analyze the effectiveness of replacing only appearing tokens instead of all tokens. The index range of replaced tokens is denoted as $[X, |\mathcal{V}|]$, and the number of tokens appearing in $[X, |\mathcal{V}|]$ satisfies $\min(\alpha\% * |\mathcal{V}|, |\mathcal{V}_{[task]})$, as required in Section 5.3.

Results for BART+DefinitionEMB are reported in Table 30. When replacing only appearing tokens, the model achieves higher ROUGE scores than when replacing all tokens. Specifically, ROUGEL-F1 improved by 0.17 and 0.08 for Y-BIGPATENT and Billsum, respectively. This difference may be caused by the varying token frequencies in the training sets. Table 31 shows the ablation study with respect to the replacing strategies for Baseline+DefinitionEMB on the MRPC test set. When replacing only appearing tokens, both RoBERTa and BART yield higher accuracy scores.

H Insights into Rare Tokens in Fine-tuned Models

This section analyzes whether fine-tuned models can distinguish rare tokens and effectively extract their semantics during text generation.

H.1 Probing Numeric-related Semantics.

Label	# of training	# of validation	# of test
Numeric <1000	836	93	72
Numeric >1000	878	98	6
Others	900	100	78
All	2614	291	156

Table 32: Numeric dataset statistics.

To investigate whether fine-tuned models can distinguish between rare numeric and non-numeric tokens and effectively extract rare numeric tokens during text generation, we conduct a probing test. Specifically, we feed tokens into a CNNDM fine-tuned model and train an additional linear classifier on the model’s final hidden layer to predict three target labels: “numeric < 1,000”, “numeric > 1,000”, and “others”. The details of the experimental settings are as follows.

Dataset. The dataset statistics for this probing test are shown in Table 32. We first introduce our test set. As mentioned in Appendix F, we added definitions for 1,252 numbers in \mathcal{V} by translating numbers into their corresponding words, such as “2” to “two”. Out of these 1,252 numbers, 78 numeric tokens start with “Ġ” and appear in the CNNDM dataset with an index greater than 40,000 in the vocabulary \mathcal{V} .⁸ We also randomly select 78 non-numeric tokens from \mathcal{V} , ensuring they start with “Ġ” and belong to the rare group within the CNNDM dataset. These 156 tokens make up our test sets.

For the training and validation sets, we first randomly select 1,000 non-numeric words from the Wiktionary dataset, ensuring that a whitespace is added at the beginning of each word. This ensures that after tokenization, the first subword token will start with “Ġ”. Similarly, we select numbers in the range [0, 1999] as our numeric words and added

⁸Note that tokens starting with or without “Ġ” are mapped into different embedding regions. Classifying both of them into the same label would place an unnecessary burden on the model during probing, so we only use those starting with “Ġ” here.

whitespace before them. These words were then divided into training and validation sets in a 9:1 ratio. We further filter the data to ensure no overlap between the training/validation and the test data.

Hyperparameters	Value
# of updates	2,810
# of warm-up updates	169
# of epochs	10
Batch size (sentences)	512
Learning rate	7e-4
Learning rate schedule	Polynomial decay
Optimizer	Adam

Table 33: Hyperparameters used for probing.

Model Settings. For both the training and validation sets, each tokenized word is fed into the encoder and decoder of the CNNDM fine-tuned model. Similarly, for the test set, each numeric or non-numeric token is processed by the encoder and decoder. Classification is performed using hidden states at the final token position in the last layer of the decoder to predict the three target labels: “numeric < 1,000”, “numeric > 1,000”, and “others”. During training, the fine-tuned parameters are frozen, and an additional feed-forward neural network is trained as the classifier. This classifier consists of two layers and is open-sourced.⁹ Table 33 lists the training parameters used for classification across the three labels.

⁹<https://github.com/facebookresearch/fairseq/blob/main/fairseq/models/bart/model.py#L294>

H.2 Sample of Summarization

Tables 34 and 35 show sample summarizations of CNNDM test set. These examples show that using DefinitionEMB helps the PLM to understand and generate rare tokens.

H.3 Isotropy of Contextual Token Representations.

Figure 20 depicts the projection of contextual token representations. That is the specific decoder layer hidden states of the token in a given context (Cai et al., 2021). Although BART + DelDirection (Figure 2 (g)) exhibits a totally different token embedding distribution from BART (Figure 2 (b)), it yields a similar contextual representations as BART. Specifically, Figures 20 (a) and (b) show that high-frequency tokens are closely grouped together based on their frequency, while low-frequency tokens are spread out in specific directions. However, when using DefinitionEMB, we observe a more concentrated distribution than BART. Its projection resembles concentric ellipses, where tokens with similar frequencies are placed in the same ellipse. This indicates that the last hidden states in DefinitionEMB involve less frequency-related information, allowing tokens of different frequencies to mix together. This finding aligns with our experimental results in Figure 5, where using DefinitionEMB enables the model to encode and extract more semantic information than both BART and DelDirection. Combing all previous experiments, we conclude that using DefinitionEMB helps the PLMs to distinguish rare tokens and effectively extract rare tokens' semantics for text generation.

Source	(CNN)For superhero fans, the cup runneth over. Most of us know the members of the Avengers by now: Iron Man, Captain America, Hulk and the rest, and the fact that a few more like Quicksilver are joining the cast in the "Avengers: Age of Ultron" sequel . But there was one character who remained a mystery: the Vision, to be played by Paul Bettany . Thus far, we've only seen his eyes in a trailer. With less than a month to go before the movie hits theaters, Marvel Studios put all the speculation to rest with a poster featuring Bettany as the heroic android , who was a member of the superhero group for many years in the comics. Meanwhile, as many Marvel fans know, Thursday was the eve of the new Netflix series "Daredevil," and after a photoshopped first look at Charlie Cox's iconic red Daredevil suit went out, Marvel put out a video of the real one . Not to be outdone, director Bryan Singer announced a new character for next year's sequel "X-Men: Apocalypse," by telling Empire magazine that Ben Hardy would be playing the role of the winged mutant Angel . He even had a photo to share. And Thursday's new super images weren't quite done, because the questions over how Jamie Bell's rocky character The Thing in the rebooted "Fantastic Four" movie (out August 7) might look were also finally answered . And he looks ... pretty much like The Thing we already knew (but reportedly, CGI this time). Within 24 hours, we got yet another indication that the superhero trend isn't going anywhere anytime soon (and we didn't even talk about the new photo of Ryan Reynolds' "Deadpool").
Reference	<u>Marvel</u> Studios releases first looks at Paul Bettany as the Vision in "Avengers: Age of <u>Ultron</u> " and Charlie Cox in full " <u>Daredevil</u> " costume . Jamie Bell's character of The Thing was also unveiled for 20th Century Fox's Marvel-based reboot of "Fantastic Four" Bryan Singer unveiled the first look at "X-Men: <u>Apocalypse</u> " Angel played by Ben Hardy .
BART	Paul Bettany will play the Vision in the "Avengers: Age of <u>Ultron</u> " sequel . The actor has been playing the <u>android</u> for many years in the comics . The "Fantastic For" reboot's" The Thing" looks pretty much like The Thing we already knew .
+DelDirection	Paul Bettany's character in "Avengers: Age of <u>Ultron</u> " is finally revealed . The actor has been playing the Vision in the comics for many years . The "Fantastic Fou" reboot's" The Thing" looks pretty much like The Thing we already knew (but CGI)
+DefinitionEMB	Paul Bettany will play the Vision in the "Avengers: Age of <u>Ultron</u> " sequel . Marvel Studios also announced a new character for "X-Men: <u>Apocalypse</u> " Ben Hardy will play the winged <u>mutant</u> Angel in "X-Men: <u>Apocalypse</u> ," director Bryan Singer said .

Table 34: Sample summarization of CNNDM test set. **Bold** in source indicates the reference-related text. Underline in reference and model outputs indicates the rare token with index larger than 40,000 in PLM's vocabulary \mathcal{V} .

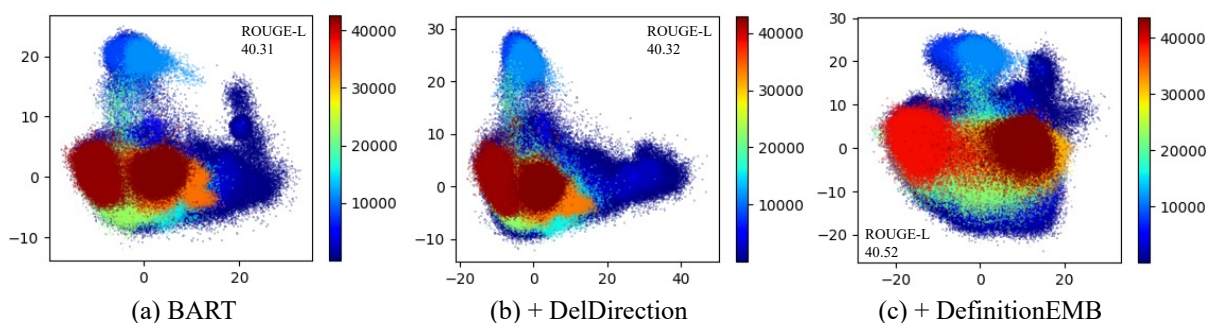


Figure 20: Projected contextual embedding in the 12th (final) decoder layer of BART-related models after fine-tuning on the CNNDM dataset. Colors indicate the token frequencies in corresponding test set.

Source	(CNN)It would have made Thomas Jefferson proud. Established on the birthday of the American founding father, Liberland – the world’s newest micronation – is founded on a firm belief in liberty and noninterference from the powers-that-be. A tiny, 7 square-kilometer parcel of land, marked on maps as Gornja Siga, its territory abuts the Danube on the border between Serbia and Croatia . The victim of a border dispute between Serbia and Croatia, it is claimed by neither side – effectively a no-man’s land. No one lives on this patch of land, which is heavily forested and contains only badly-maintained access roads and a run-down house, abandoned for decades. This is where Euroskeptic Czech politician Vit Jedlicka stepped in. On April 13 he planted his newly-designed yellow and black flag in the territory, declaring the area the Free Republic of Liberland – a tiny sliver of a country, bigger only than the Vatican and Monaco. He tells CNN that the country will be formally founded on May 1 and is inviting, through the media, the world’s heads of state to attend a formal ceremony marking the presumptive nation’s birth. He says that he will also invite 7,500 of the 300,000 applicants that applied to become citizens of Liberland to the ceremony, where he will grant them citizenship. "I will grant citizenship if they can make it to the party," he told CNN by phone. "It’s short notice but a good challenge, and also for the presidents (and other heads of state) if they can make it to the founding of our country." Jedlicka, an active member of the Czech Republic’s Party of Free Citizens, opposes excessive government interference. He says his attempts to enact change in his home country led him to the political experiment that is Liberland. "I would describe it as a global revolution. It’s just the beginning," he tells CNN via Skype. Founded on staunchly libertarian principles – its motto is "To live and let live" – its website describes its system of governance as being a "constitutional republic with elements of direct democracy." It will use a form of cryptocurrency – similar to Bitcoin – as its national currency, bypassing the need for a central bank and will, according to its constitution, keep government’s noses out of everything possible, from the banks to prostitution. "Liberland prides itself on personal and economic freedom of its people, which is guaranteed by the Constitution, which significantly limits the power of politicians so they could not interfere too much in the freedoms of the Liberland nation," the world’s newest constitutional document states. Financial regulation will be minimal, if at all present. Jedlicka says almost 300,000 applications for citizenship have been received , about 20 of which have been accepted. "Thousands of Americans, Swiss people. Also a lot of Arabic peoples who feel oppressed by the regimes there." He envisions, ultimately, a community of around 35,000 Liberlanders, not all of whom will be full-time residents. He says he expects trouble from his neighbors, whose land he has effectively annexed. "From Serbia, Croatia, we expect some trouble but we expect international laws will applied and any movement against us would be an attack on a sovereign nation, and we will offer nothing but passive resistance. For now, (though) we will make roads, docks." For its part, the Serbian Ministry of Foreign Affairs released a statement to CNN that stated that Liberland would not theoretically impinge upon its border, which is delineated by the Danube, but "the Ministry also considers this a frivolous act which needs no further comment." Croatia’s counterpart was similarly dismissive. "Virtual quips, however interesting they occasionally sound, remain what they are – virtual quips, and for them we have no official comment."
Reference	Vit Jedlicka, the first president of Liberland, tells CNN that the country will be formally founded on <u>May 1</u> . On <u>April 13</u> , Jedlicka declared an area between Croatia and Serbia "the Free Republic of Liberland" Jedlicka says that almost <u>300,000</u> applications for citizenship have so far been received .
BART	Liberland is a tiny, <u>7</u> square-kilometer parcel of land, marked on maps as Gornja Siga, which abuts the Danube on the border between Serbia and Croatia . The land is claimed by neither Serbia or Croatia, and is effectively a no-man’s land . Czech politician Vit Jedlicka planted his newly-designed yellow and black flag in the territory, declaring the area the Free Republic of Liberland . He says he expects trouble from his neighbors, whose land he has effectively annexed .
+DelDirection	Czech politician Vit Jedlicka has declared the Free Republic of Liberland, a tiny sliver of land on the border of Serbia and Croatia . He says he expects trouble from his neighbors, whose land he has effectively annexed . "I would describe it as a global revolution. It’s just the beginning," he tells CNN .
+DefinitionEMB	Czech politician Vit Jedlicka has declared the Free Republic of Liberland, a tiny sliver of land on the Serbian-Croatian border . He says he will grant citizenship to <u>7,500</u> of the <u>300,000</u> applicants who applied to become citizens of Liberland . "I would describe it as a global revolution. It’s just the beginning," says Jedlicka via Skype .

Table 35: Sample summarization of CNNDM test set. **Bold** in source indicates the reference-related text. Underline in reference and model outputs indicates the numeric in PLM’s vocabulary √.